The osteology of *Ferrodraco lentoni*, an anhanguerid pterosaur from the mid-Cretaceous of Australia

Adele H. Pentland, Stephen F. Poropat, Matt A. White, Samantha L. Rigby, Joseph J. Bevitt, Ruairidh J. Duncan, Trish Sloan, Robert A. Elliott, Harry A. Elliott, Judy A. Elliott & David A. Elliott

Check for updates

ARTICLE

THE OSTEOLOGY OF *FERRODRACO LENTONI*, AN ANHANGUERID PTEROSAUR FROM THE MID-CRETACEOUS OF AUSTRALIA

ADELE H. PENTLAND, [1,2*] STEPHEN F. POROPAT, [1,2] MATT A. WHITE, [2,3] SAMANTHA L. RIGBY, [1,2] JOSEPH J. BEVITT,[4] RUAIRIDH J. DUNCAN, [5] TRISH SLOAN,[2] ROBERT A. ELLIOTT,[2] HARRY A. ELLIOTT,[2] JUDY A. ELLIOTT,[2] and DAVID A. ELLIOTT[2]

[1]School of Science, Computing and Engineering Technologies, Swinburne University of Technology, John St, Hawthorn, Victoria 3122, Australia, apentland@swin.edu.au, sporopat@swin.edu.au, srigby@swin.edu.au;
[2]Australian Age of Dinosaurs Natural History Museum, The Jump-Up, Winton, Queensland 4735, Australia, pentlandadele@gmail.com, stephenfporopat@gmail.com, trish.sloan@aaod.com.au, bobelliott88@bigpond.com, harry.a.elliott@gmail.com, judy.elliott@aaod.com.au, david.elliott@aaod.com.au;
[3]School of Environmental and Rural Science, University of New England, Armidale, New South Wales 2351, Australia, mwhite62@une.edu.au;
[4]Australian Centre for Neutron Scattering, Australian Nuclear Science and Technology Organisation, Sydney, NSW 2234, Australia, jbv@ansto.gov.au;
[5]School of Biological Sciences, Monash University, Melbourne, Victoria 3800, Australia, ruairidh.duncan@monash.edu

ABSTRACT—*Ferrodraco lentoni*, an anhanguerid from the Upper Cretaceous Winton Formation of northeast Australia, is the most complete Australian pterosaur described to date, represented by a partial cranium, incomplete cervical series and wing elements. Herein we present a comprehensive osteological description of *Ferrodraco*, as well as an emended diagnosis for this taxon. In addition, we compare *Ferrodraco* with other isolated pterosaur remains from Australian Cretaceous deposits. Subtle, yet salient, differences indicate that at least three of these specimens, all derived from the upper Albian Toolebuc Formation, are distinct from *Ferrodraco*. However, we are uncertain whether these specimens are attributable to *Mythunga camara*, *Aussiedraco molnari*, *Thapunngaka shawi*, or an as yet un-named taxon. Detailed description of the postcranial material of *Ferrodraco* also provides an opportunity to reassess its phylogenetic position. In one analysis, *Ferrodraco* and *Mythunga* are resolved as sister taxa within Tropeognathinae, whereas in another, *Ferrodraco*, *Mythunga*, and *Tropeognathus* form a polytomy within Coloborhynchinae. Either way, these slight differences notwithstanding, a close relationship between *Ferrodraco* and *Mythunga* is evident, supporting the interpretation that they form a clade. By contrast, *Aussiedraco molnari* is resolved as a member of Targaryendraconia, a clade with a cosmopolitan distribution. The presence of several anhanguerian taxa or lineages in the late Early and early Late Cretaceous of northeast Australia is suggestive of even greater diversity in the Australian pterosaur fauna.

SUPPLEMENTAL DATA—Supplemental materials are available for this article for free at www.tandfonline.com/UJVP.

INTRODUCTION

The Australian pterosaur fossil record is depauperate when compared with that of the rest of the world. Fewer than 20 specimens have been formally described, with the majority consisting of isolated and fragmentary remains assigned to Ornithocheiridae sensu Unwin (2003), equivalent to Anhangueridae sensu

Holgado and Pêgas (2020) and Anhangueria sensu Andres et al. (2014). Moreover, the first Australian pterosaur material was not formally described until 1980 (Molnar and Thulborn, 1980). This is far more recent than the earliest reports of pterosaur remains from Europe (Collini, 1784; Cuvier, 1809) or North America (Cope, 1871; Marsh 1872, 1876), but also more recent than the first reports from every other continent, bar one. Possible pterosaur material from South America was alluded to as early as the early 1900s (Mawson and Smith Woodward, 1907; Rodrigues and Kellner, 2010), but the first description of pterosaur remains from that continent was not published until the 1950s (Price, 1953). The first pterosaur material from Africa was described in the 1930s (Reck, 1931; Unwin and Heinrich, 1999), whereas the first unequivocal Asian pterosaurs were identified in the 1960s (Young, 1964). Although the earliest report of a pterosaur from India (Dubey and Narain, 1946) was called into question by Colbert (1969) and Jain (1974), the latter author also described the first unambiguous pterosaur material from India in the 1970s. The only

continent for which the earliest report of a pterosaur post-dates that of Australia is Antarctica (Hammer and Hickerson, 1994), with only two isolated and fragmentary wing bones described since this initial report (Kellner et al., 2019). Thus, Australian pterosaur research is still in its infancy when compared with almost every other continent.

All pterosaur specimens presently known from Australia date to the Cretaceous. Unfortunately, attempts to elucidate the taxonomic diversity of the Australian pterosaur record have been hampered by the incomplete and isolated nature of these remains. At present, four pterosaur taxa have been recognized from Australia, three of which derive from the upper Albian Toolebuc Formation. These are the anhanguerid *Mythunga camara* (Molnar and Thulborn, 2007; Pentland and Poropat, 2019); the targaryendraconid *Aussiedraco molnari* (Kellner et al., 2011; Pêgas et al., 2019) and the recently described *Thapunngaka shawi* (Richards et al., 2021). Whereas *Mythunga*, *Aussiedraco*, and *Thapunngaka* were established on the basis of incomplete cranial material, *Ferrodraco* is the most complete pterosaur taxon recognized from Australia, with 10% of the skeleton preserved (AODF 876). Furthermore, this taxon provides significant morphological data and sheds light on the evolution and taxonomic diversity of pterosaurs from Australia. Herein, we present a full osteological description of *Ferrodraco* with an emphasis on elements only briefly mentioned in the holotype description (Pentland et al., 2019). In addition, we reassess the phylogenetic position of this taxon using recently published phylogenetic datasets.

Institutional Abbreviations—**AAOD**, Australian Age of Dinosaurs Natural History Museum, Winton, Queensland, Australia; **AODF**, Australian Age of Dinosaurs Fossil; **AODL**, Australian Age of Dinosaurs Locality; **AMNH**, American Museum of Natural History, New York, U.S.A.; **BSP**, Staatliche Naturwissenschaftliche Sammlungen Bayerns – Bayerische Staatssammlung für Paläontologie und Geologie, Munich, Germany; **FSAC**, Faculté des Sciences Aïn Chock, Université Hassan II, Casablanca, Morocco; **MN**, Museu Nacional, Rio de Janeiro, Brazil; **NHMUK**, (=BMNH) Natural History Museum, London, United Kingdom; **QMF**, Queensland Museum Fossil, Australia; **RGM**, National Natuurhistorisch Museum, Leiden, the Netherlands; **SAO**, Sammlung Oberli, St. Gallen, Switzerland; **UWPI**, Paläontologisches Institut der Universität Wien, Vienna, Austria.

METHODS

Synchrotron Scanning

Microtomographic reconstruction of AODF 876 was achieved by scanning each element individually, employing the Imaging and Medical Beamline (IMBL) at the Australian Nuclear Science and Technology Organisation's (ANSTO) Australian Synchrotron, Clayton, Victoria, Australia. Each sample was mounted vertically on the rotation stage, and radiographs acquired as the samples were rotated about their vertical axes.

For the ulna, a cubic voxel size of 31 mm and a monochromatic beam energy of 85 keV was utilized; for the snout tip, the voxel size was 41 mm. For all other bones, a voxel size of 31 mm and beam energy of 90 keV was used. Experimental variables were adjusted to suit the particular bone geometry, attenuation, and contrast.

X-rays were converted to visible photons and detected using 'Ruby', a 20 mm thick GdO/CsI(Tl)/CdWO$_4$ scintillator screen coupled with a PCO.edge sCMOS camera (16-bit, 2560 × 2160 pixels) and a Nikon Makro Planar 50 mm lens. A total of 1800 equally spaced angle shadow-radiographs with an exposure length of 0.3 s were obtained every 0.10° as the sample was continuously rotated 180° about its vertical axis. Due to limited beam

height, successive sets of radiographs were obtained with a vertical displacement of 25 mm between each tomographic dataset to fully cover each sample. One hundred dark (closed shutter) and beam profile (open shutter) images were obtained for calibration before initiating shadow-radiograph acquisition. The raw 16-bit radiographs were spot-filtered and a median filter of radius 0.8 pixels applied in ImageJ prior to normalization and stitching of the limited-height tomographs using IMBL Stitch, the in-house software, and 16-bit three-dimensional reconstructions achieved using Octopus Reconstruction v8.8 and the filtered-back projection algorithm.

The resulting images were imported into Dragonfly 2021.1 (Object Research Systems (ORS) Inc, Montreal, Canada, 2020) and converted into 3D surface meshes of each individual bone. Owing to the size of the datasets, a maximum of 500 images were processed at any one time, which required many specimens' meshes to be digitally sutured together. During 3D mesh creation, residual fine meshes, not associated with the targeted specimen, were often created in error. To get rid of these residual meshes the entire mesh was exported as an OBJ file and imported into Rhinoceros 5.0 (Robert McNeel and Associates, California, U.S.A.). The explode tool separated each mesh which enabled the targeted specimen mesh to be selected and hidden, leaving the unwanted mesh visible; these were subsequently selected and deleted. The targeted mesh was then made visible and exported as an OBJ file. These meshes were imported into Zbrush 2021.6.2 64bit Pixologic (Pixologic Inc, California, U.S.A.), which was used to digitally suture separate meshes that constituted an individual specimen. Zbrush was also used to visually articulate bones and create 3D movies of the specimens.

Phylogenetic Approach

The phylogenetic positions of *Ferrodraco* and *Mythunga* were reassessed by conducting a phylogenetic analysis using a modified version of the datasets of Pêgas et al. (2019) and Holgado and Pêgas (2020). The Holgado and Pêgas (2020) dataset was modified by revising scores for *Ferrodraco*, *Mythunga*, and *Aussiedraco*, and these changes are detailed in the supplementary material. The Pêgas et al. (2019) dataset was modified by including *Ferrodraco* and *Mythunga* and revising scores for *Aussiedraco*, based on personal observation of the *Aussiedraco* holotype specimen (by A.H.P. and S.F.P., 2018). Including our modifications, the Pêgas et al. (2019) dataset contains 160 discrete characters and 71 taxa, whereas the Holgado and Pêgas (2020) dataset contains 179 discrete characters and 74 taxa.

Phylogenetic analyses were run in TNT v.1.5 (Goloboff et al., 2008) following the methodology employed by Pêgas et al. (2019) and Holgado and Pêgas (2020), respectively. Following Pêgas et al. (2019) and Holgado and Pêgas (2020), we ran a search for the most parsimonious trees (MPTs) via Traditional Search (TBR swapping algorithm), 10,000 replicates, random seed, and collapsing trees after search. We ran Parsimony analyses and applied equal weighting of characters for both datasets using the heuristic tree search, with no additive characters considered. As per Holgado and Pêgas (2020), our analysis was conducted via New Technology, to recover the island with the minimum length trees (MLTs). Parameters of this analysis are as follows: "Sectorial Search, ratchet (parameters: 20 substitutions made, or 99% swapping completed, six up-weighting prob., six down-weighting prob., and a total number of iterations of 10), tree fusing, Driven search (15 initial addseqs., 15 times of min. length), random seed, and without collapsing trees after search" (p. 3). The results of the New Technology analysis were subjected to a Traditional Search (TBR swapping algorithm), starting with trees from RAM, and without collapsing trees after search. Fifteen most parsimonious trees (MPTs) with a

minimum length of 415 steps were generated (consistency index [CI]: 0.631; retention index [RI]: 0.868). As per Pêgas et al. (2019), our analysis was conducted via New Technology and set with the following parameters: "Sect. Search, Ratchet (parameters: 20 substitutions made, or 99% swapping completed, 6 upweighting prob., 6 down-weighting prob., and a total number of iterations of 10), Tree fusing, Driven search (15 initial addseqs., 15 times of min. length), random seed, and without collapsing trees after search" (p. 2). The New Technology results were then analysed via Traditional Search (TBR swapping algorithm), starting trees from RAM, and without collapsing trees after search. Our phylogenetic analysis by parsimony produced 15 MPTs with a minimum length of 393 steps with CI of 0.623 and RI of 0.865.

In instances where a specific character is referred to, the dataset is referenced appropriately, with character 95 referred to as (C95), character 98 referred to as (C98), and so on. Character numbers are referenced here as they appear in the software Mesquite 3.6 (Maddison and Maddison, 2018), not as they appear when referenced in supplementary material (i.e., the first character is C0, not C1).

Depositional Setting

The type locality for *Ferrodraco lentoni* is AODL 245 (the "Pterosaur Site"), which is located near Wardoo Creek on Belmont Station, east-northeast of Winton, central Queensland, Australia (Fig. 1). Fossil remains of *Ferrodraco* are three-dimensionally preserved and were recovered from the transition zone between a layer of overburden consisting of cracking clays or "black soil" (Gray et al., 2002; Jell, 2013) overlying fine-grained mudstone of the Winton Formation. This, in turn, overlies a layer of fine-grained, ferruginous sandstone. Sediments at AODL 245 were deposited within a distal crevasse splay setting, in a low-energy environment preserving intermittent sandstone and siltstone, with the coarsest layer represented by an iron-rich fine sand. Macrofloral remains were not found in association with AODF 876; however, small fragments of silicified wood (ranging from 20–50 mm) were observed high in the sequence. An ichnite fauna comprising inclined tubular burrows with backfill was observed at the base of the sand layer.

The distal end of the left ulna, distal end of the left radius, fragments of the mandible, a partial tooth, partial left scapulocoracoid, distal end of the left metacarpal IV and other fragments were found scattered at the surface. The premaxilla, maxilla, premaxillary crest, and parts of the first wing phalanx were discovered in the transition zone between the weathered soil profile and a fine-grained mudstone, which in turn overlies a layer of fine-grained sandstone. The cervical vertebrae, mandibular symphysis, and frontal were recovered within the dry creek bed. The shaft and distal end of left metacarpal IV were found in association with the proximal end of right metacarpal IV and were recovered within the transition zone between the Quaternary overburden and Cretaceous mudstone. The shaft of both metacarpal IVs and the distal end of the left ulna (distal to the pneumatic foramina) show some signs of crushing.

Although fragments of individual bones were scattered some distance from the main concentration of fossil material, some elements found separately keyed into others. This includes the occluded and interlocked premaxilla–maxilla and mandibular symphysis, the ulna and radius (with cortical bone from the ulna preserved on the radius, based on synchrotron data), the left metacarpal IV and the proximal end of the first wing phalanx (with the extensor tendon process fused), and a fragmentary non-flight metacarpal in ironstone with the posterior surface of the left metacarpal IV. Given that no other vertebrate fossils were recovered at the site, and that all specimens are size congruent with no duplication of elements, the remains described

herein can be confidently assigned to a single individual. Moreover, the absence of other faunal remains at the site, as well as the scarcity of ichnites and plant material relative to other sites in the Winton Formation, lends support to the interpretation that these remains can be attributed to a single pterosaur.

SYSTEMATIC PALEONTOLOGY

PTEROSAURIA Kaup, 1834
PTERODACTYLOIDEA Plieninger, 1901
PTERANODONTOIDEA Marsh, 1876 sensu Kellner, 2003b
ANHANGUERIA sensu Rodrigues and Kellner, 2013
ANHANGUERIDAE Campos and Kellner, 1985
FERRODRACO LENTONI Pentland, Poropat, Tischler, Sloan, Elliott, Elliott, Elliott, and Elliott 2019

Holotype—AODF 876. As defined in the original description, "anterior portion of skull consists of partial premaxillae, maxillae and dentaries (including premaxillary and mandibular crests and the mandibular symphysis); partial left frontal; left mandibular articular region including the surangular, angular and articular; five partial cervical vertebrae; partial right scapulocoracoid; partial left ulna; partial left radius; left proximal, distal and lateral carpals; left metacarpal IV; proximal end of right metacarpal IV; fragmentary left non-wing manual phalanges; partial left first wing phalanx (IV-1); and associated fragments" (Pentland et al., 2019, p. 2).

Type Stratum—Winton Formation; Cenomanian–lowermost Turonian (Tucker et al., 2013).

Type Locality—The 'Pterosaur' Site, AODL (Australian Age of Dinosaurs Locality) 245, Belmont Station, northeast of Winton, Queensland, Australia.

Diagnosis—Anhanguerid diagnosed by the following autapomorphies: (1) first tooth pair of the premaxilla and mandible smaller than all other teeth anterior to the mandibular symphysis; (2) fourth through seventh teeth smaller than the third and eighth.

DESCRIPTION AND COMPARISONS

Skull

The skull is incomplete, with the largest preserved portion comprising the anterior section of the skull. This includes the anterior portion of the premaxilla–maxilla and premaxillary crest, as well as parts of the mandible including the mandibular symphysis and partial dentary crest (Figs. 2, 3, S1 and S2). The fact that one fragment of the jaw preserves the upper and lower jaws in occlusion implies that the skull was articulated during fossilization. The only identifiable elements from the posterior part of the skull include part of the frontal and a fragment preserving the fused surangular and angular. Additional jaw fragments bearing small, oval alveoli were also recovered during excavation; however, it cannot be determined whether these derive from the upper or lower jaw (Fig. S3).

Ferrodraco differs from other members of the Anhangueridae in that the anterior part of the skull is not laterally expanded (Kellner, 2003a). In this regard, *Ferrodraco* is more similar to members of the Targaryendraconia (Pêgas et al., 2019). However, *Ferrodraco* differs from targaryendraconians in that the width of the mandibular symphysis is over three times that the alveolar diameter, whereas in the latter, the symphysis is subequal to three times the alveolar diameter (Pêgas et al., 2019). *Ferrodraco* possesses a dorsal deflection of the palatal tip, such that the angle relative to the rest of the palate is less than 90°. In anterior view, the first pair of premaxillary teeth in *Ferrodraco* are positioned slightly dorsal to the rest of the tooth row. By
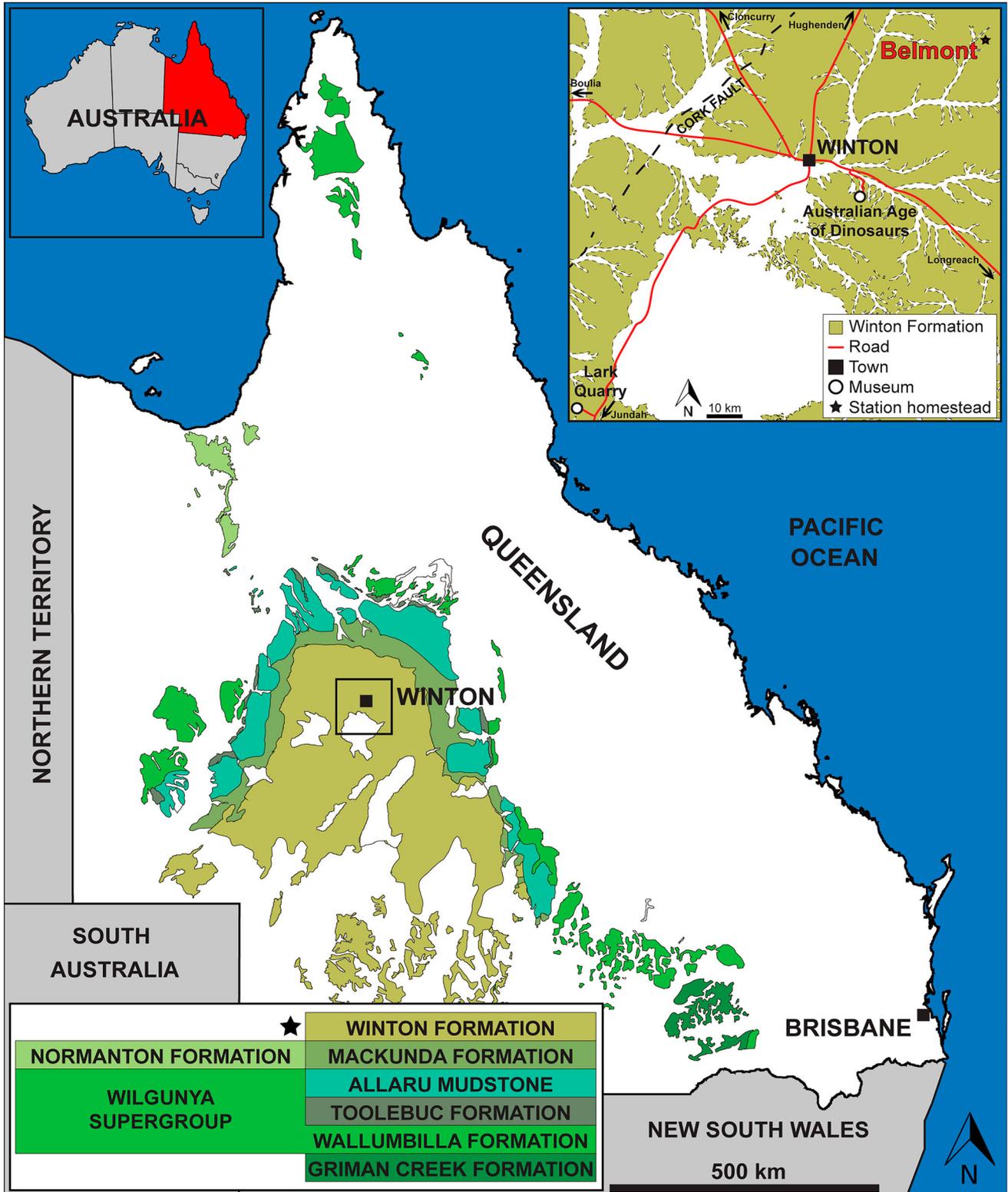
FIGURE 1. Map of Queensland, Australia showing the distribution of surface exposures of Cretaceous sediments in Queensland, the location of the town of Winton and museums in the region, and the location of Belmont Station where the holotype and only known specimen of *Ferrodraco lentoni* was discovered. This map was drafted by S.F.P. in Adobe Illustrator CC 2017, and includes geological information summarized from Vine and Jauncey (1964) and Vine et al. (1967). (© Commonwealth of Australia [Geoscience Australia] 2019. This product is released under the Creative Commons Attribution 4.0 International License [creativecommons.org/licenses/by/4.0/legalcode].)
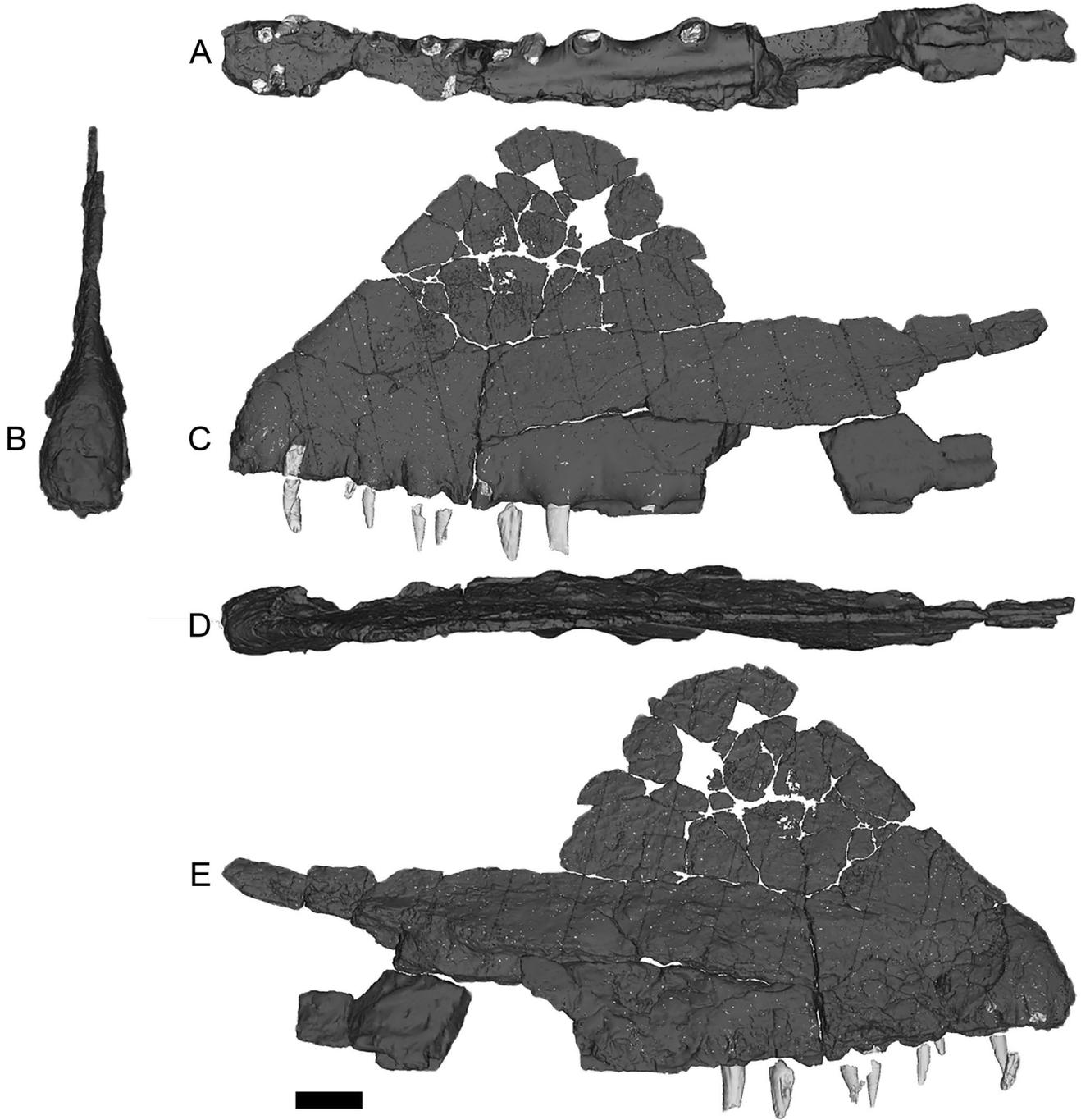
FIGURE 2. *Ferrodraco lentoni* holotype skull AODF 876 from the Winton Formation of Queensland, Australia. Some adherent ironstone matrix has been digitally removed. Three-dimensional surface renders of the premaxilla–maxilla in **A**, ventral; **B**, anterior; **C**, left lateral; **D**, dorsal; and **E**, right lateral views. All 3D renders by M.A.W. Scale bar equals 20 mm.

contrast, these teeth are situated even further dorsally in *Coloborhynchus clavirostris* (NHMUK PV R 1822) and *Uktenadactylus wadleighi*. *Uktenadactylus* differs from *Ferrodraco* in that a prominent depression is present in the former, dorsal to the first pair of premaxillary teeth on the anterior part of the skull (Lee, 1994). By contrast, a depression ventral to the first pair of premaxillary teeth is present in *Coloborhynchus clavirostris* (Kellner et al., 2013). Although the anteriormost teeth of the premaxilla in *Ferrodraco* are vertically oriented, synchrotron scan

data reveal that the corresponding replacement teeth are procumbent and in close proximity to the second pair of replacement teeth (Fig. 2; Fig. S2). *Ferrodraco* is similar to many members of the Anhangueridae (Jacobs et al., 2019) in that the deltoid facet has a dorsoventral height subequal to, or less than its transverse width. Based on their alveolar diameters, the first premaxillary teeth have a sub-circular cross-section, but do not appear enlarged. In this regard, *Ferrodraco* differs from most other anhanguerids (Campos and Kellner, 1985), with the exception
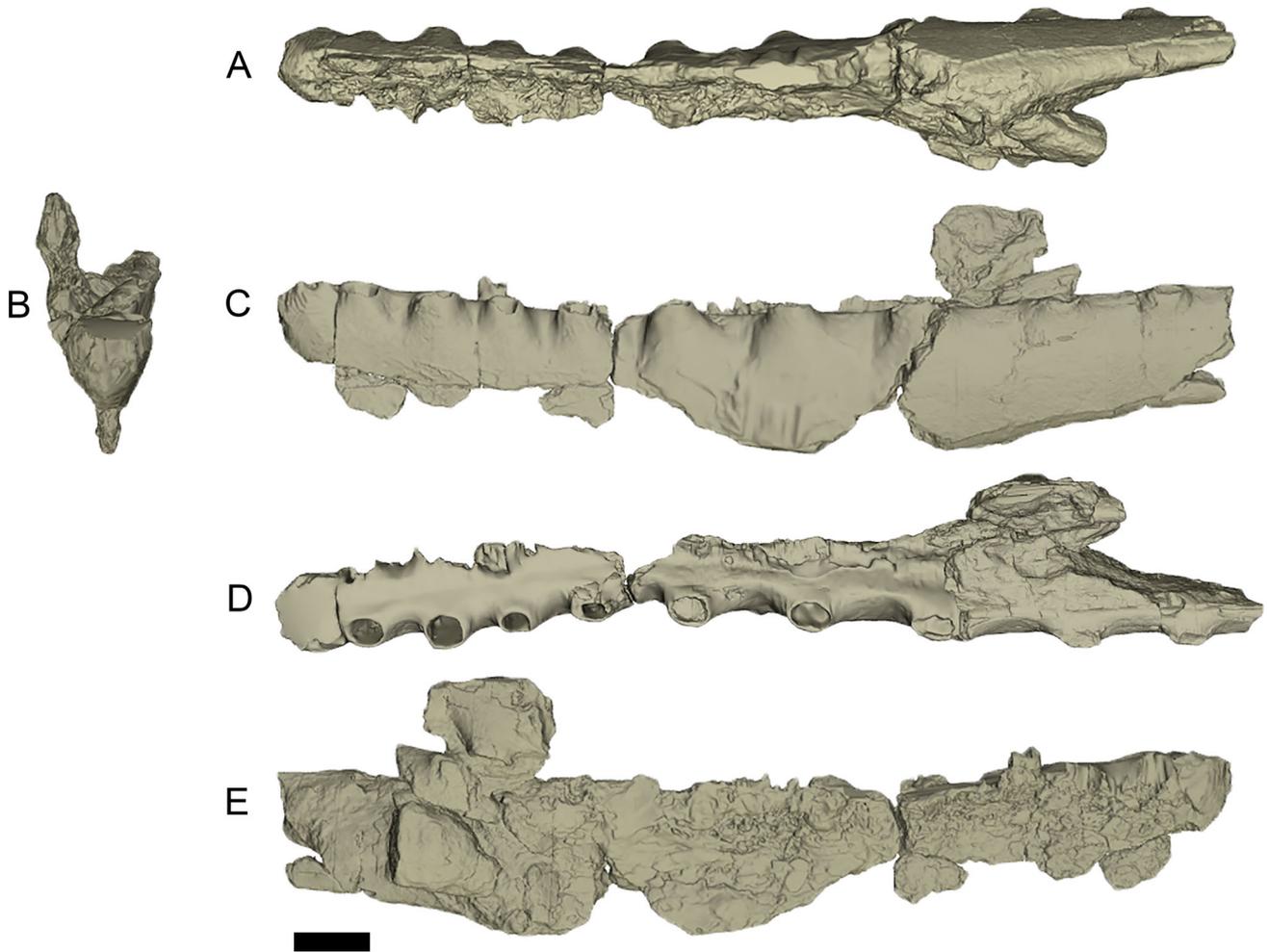
FIGURE 3. *Ferrodraco lentoni* holotype mandible AODF 876. Three-dimensional surface renders of the mandible in **A**, ventral; **B**, anterior; **C**, left lateral; **D**, dorsal; and **E**, right lateral views. All 3D renders by M.A.W. Scale bar equals 20 mm.

of *Siroccopteryx moroccensis* in which the first tooth pair of the premaxilla are not enlarged (Mader and Kellner, 1999). The position of the second pair of premaxillary teeth relative to the third cannot be determined with certainty because of adherent ironstone. Unfortunately, the only tooth occupying alveolus 3 was a replacement tooth in right lateral view, based on synchrotron data (Fig. S2). Moreover, based on the dimensions of the alveoli (Table 1), we provisionally suggest that the third tooth pair on the premaxilla–maxilla is double the size of the fourth tooth pair. Based on the left lateral surface of the premaxilla–maxilla, the fifth tooth pair does not appear medially displaced relative to the adjacent alveoli. In both the premaxilla–maxilla and mandible, the third tooth pair is larger than the fourth, based on their alveolar diameters (Table 1). This differs from *Liaoningopterus gui*, in which the fourth tooth of the premaxilla–maxilla was the largest (Wang and Zhou, 2003). Given that the right lateral surface of the skull is incomplete, it cannot be determined with certainty whether the first three teeth pairs on either the upper or lower jaws are more closely spaced than subsequent teeth (Table 2). Based on the alveolar diameters, we infer that the teeth occupying the fourth tooth position were smaller than those in the fifth and sixth tooth positions.

In palatal view, the lateral margins of the anterior end of the premaxilla are rounded, when compared with those of *Siroccopteryx*, a taxon noted for having a quadrangular expansion of the premaxilla (Rodrigues and Kellner, 2008). Unfortunately, the anterior margin of the nasoantorbital fenestra in *Ferrodraco* is not preserved. Thus, it cannot be determined with certainty whether the palate is laterally expanded at the level of the anterior margin of the nasoantorbital fenestra. Moreover, there is no indication of a bulbous projection on the palate between the second premaxillary teeth. Although the palate is largely incomplete, a palatal ridge is present in *Ferrodraco* between the 2nd and 4th alveoli, and this corresponds to a groove on the mandible. Therefore, a palatal ridge is present anterior to the fifth tooth position. If the assumption that the mandibular groove accommodates the palatal ridge is correct, then, based on synchrotron data, this feature becomes more pronounced posteriorly, as in *Tropeognathus mesembrinus* (Wellnhofer, 1987). By contrast, the palatal ridge in *Siroccopteryx* initiates level with the posterior margin of the fifth alveoli and is transversely wider relative to the palatal ridge of *Ferrodraco* (Mader and Kellner, 1999).

The premaxillary crest is laterally thin, consisting of two individual plates separated by trabeculae. Unfortunately, the premaxillary crest was damaged prior to collection. As such, sections of the crest are missing, and the posterior margin is incomplete. Based on what is preserved of the premaxilla, it is clear that the premaxillary crest is confined to the anterior third of the skull. The presence of a large, blade-like premaxillary crest

TABLE 1. Measurements of the alveolar diameters observed in *Ferrodraco lentoni* (AODF 876) in millimeters. Measurements based on incomplete alveoli are indicated with an asterisk (*).

Element	Alveolus	Mesiodistal length (mm)	Labiolingual width (mm)	Observations
Left premaxilla–maxilla	1	1.5	1	
	2	4	3.5	
	3	N/A	N/A	Alveolus infilled with ironstone
	4	3.5	2	
	5	6	4	
	6	5	5	Alveolus preserved as two separate fragments of jaw
	7	9	N/A	Alveolus occupied by tooth, labiolingual width cannot be determined
	8	8	8	
Left dentary	1	2	1.5	
	2	4	3.5	
	3	8		Lingual surface partially obscured by ironstone
	4	6	3	
	5	6	4	
	6	7	6	
	7	7	6	
	8	9	N/A	Jaw tightly occluded; lingual surface partially obscured by ironstone
	9	5	1.5	
	10	4	1	
	11	3	1	
	12	2	1	
	13	N/A	N/A	Left dentary incomplete
	14	1.5	0.5	
Right premaxilla–maxilla	1	2.5	1.5	Measurement taken from the base of the preserved tooth
	2	3	2	Measurement taken from the base of the preserved tooth
	3	6*	5*	Posterior and lateral margins incomplete; measurement taken based on outer margin preserved in ironstone
	4			
	5			
	6			
	7			
	8			
	9			
Right dentary	1	2	1.5	
	2	4	N/A	Partial tooth occupying alveolus, incomplete on the right lateral surface
	3	N/A	N/A	
	4	N/A	N/A	
	5	N/A	N/A	
	6	N/A	N/A	
	7	N/A	N/A	
	8	N/A	N/A	
	9	N/A	N/A	

differentiates *Ferrodraco* from other anhanguerians which lack crests, such as *Liaoningopterus gui* (Wang and Zhou, 2003), *Ludodactylus sibbicki* (Frey et al., 2003), *Guidraco venator* (Wang et al., 2012) and *Cearadactylus atrox* (Vila Nova et al., 2014). The premaxillary crest of *Ferrodraco* is confluent with the anterior margin of the skull, and thus differs from *Anhanguera blittersdorffi* (Wellnhofer, 1987), *Anhanguera* sp. (AMNH 22555; Wellnhofer 1991c) and *Anhanguera piscator* (Kellner and Tomida, 2000). In this regard, *Ferrodraco* is more similar to *Siroccopteryx* but differs in that the anterior margin of the premaxillary crest of *Ferrodraco* rises steeply and is laterally compressed (Mader and Kellner, 1999). The premaxillary crest slopes posterodorsally at ca. 60° (Pentland et al., 2019), whereas the slope in *Tropeognathus mesembrinus* is ca. 70° based on observation of the schematic published by Wellnhofer (1987).

The left lateral surface of the skull in *Ferrodraco*, including the premaxillary crest is smooth and lacks ridges, channels or nutrient foramina. On the anterior margin of the mandible, a small rugose surface is present (Pentland et al., 2019:fig. 4k). Although the taxonomic significance of such rugose surfaces, nutrient foramina, ridges, and channels on anhanguerian pterosaur skulls is unclear, it is worth noting variation in these structures and their distribution among taxa within Anhangueria. Mader and

Kellner (1999) observed rugosities, meandering striations, and shallow pits on the holotype and only known specimen of *Siroccopteryx moroccensis*. At least some of these surface features were attributed to the presence of an abscess, supported by the swelling of the bone on the left maxilla near alveoli four and five (Mader and Kellner, 1999). Mader and Kellner (1999) also observed holes near these tooth loci and suggested that they might have allowed for drainage of an abscess. Veldmeijer (2003) also noted a network of small channels, most less than 1 mm wide, restricted exclusively to the premaxillary crest of *Anhanguera spielbergi* (RGM 401 880). Several small pits, with diameters typically less than 1 mm, were also noted on the oblique surface of the premaxillary crest. Nutrient foramina were observed on both the maxilla and dentary of *Mythunga*, with a foramen positioned distal to the base of several dentary teeth (Pentland and Poropat, 2019). Several shallow, anteroventrally–posterodorsally inclined channels were also observed on the maxilla of *Mythunga*, and a longer channel was identified on the dentary (Pentland and Poropat, 2019:fig. 4b). Shallow channels were also observed on the incomplete maxilla of MN 6594-V (referred to *Tropeognathus* cf. *T. mesembrinus*), and interpreted as impressions of blood vessels (Kellner et al., 2013). It has been suggested that these served as a cooling

TABLE 2. Interalveolar spacing of Ferrodraco lentoni (measurements taken at apex of alveoli).

Left premaxilla–maxilla	Mesiodistal length of interalveolar space (mm)
1–2	3
2–3	6
3–4	5
4–5	3
5–6	8
6–7	10
7–8	17
Left dentary	
1–2	5
2–3	6
3–4	4
4–5	6
5–6	9
6–7	15
7–8	16
8–9	22
9–10	14
10–11	13
11–12	11
Right premaxilla–maxilla	
n+1–2	3
n+2–3	6
Right dentary	
n+1–2	6

mechanism, based on comparisons with the tapejarid *Thalassodromeus* (Kellner et al., 2013). Pinheiro and Rodrigues (2017) also noted foramina located on the alveolar borders of several maxillary teeth of *Anhanguera* sp. (AMNH 22555), specifically on the lingual surface of the 7th–10th tooth pairs. More recently, Jacobs et al. (2019) noted several foramina present on the occlusal surface, lingual to the alveoli, on FSAC-KK 5005, a partial mandibular symphysis from the Kem Kem Beds, referred to *Anhanguera* cf. *A. piscator*.

The preserved part of the mandible of *Ferrodraco* includes the fused mandibular symphysis, the anterior part of the left ramus and parts of the right ramus. The anterior end of the mandibular symphysis is rounded, lacking an anteriorly projected dentary tip and odontoid process. Unfortunately, parts of the right lateral surface of the mandible have been eroded. The ventral margin of the mandibular symphysis is incomplete, with only parts of the dentary crest preserved. Moreover, based on comparisons with the premaxillary crest, the mandibular crest is similar to other members of the Anhangueridae, in that it is 'blade-like' and transversely thin, made up of plates of bone separated by trabeculae. The transverse width of the anterior part of the dentary in *Ferrodraco* is four times the width of the alveoli. Although only part of the left mandibular ramus is preserved in *Ferrodraco*, it remains relatively straight (Pentland et al., 2019:fig. 3d), thereby differing from the diverging mandibular rami observed in *Anhanguera spielbergi* and "*Anhanguera robustus*" (BSP 1987 I 47; based on photographs sent to us by O. Rauhut; Fig. S4). Based on synchrotron data, the mandibular groove begins posterior to the second mandibular tooth pair (Fig. 3). This groove varies in depth and transverse width (Pentland et al., 2019:fig. 4f), becoming both dorsoventrally deeper and transversely wider posteriorly, and appears most prominent anterior to the mandibular symphysis. By contrast, the mandibular groove in "*Anhanguera robustus*" extends to the tip of the mandible (Fig. S4H).

Based on the preserved parts of the skull and alveoli therein, the teeth were distributed evenly along the jaws, as evidenced by the alveoli. Although both the maxilla and mandible are incomplete, the left dentary preserves the longest continuous sequence of alveoli (14) and demonstrates that tooth size decreases posteriorly from the 9th alveolus (Table 1). Moreover, the mesiodistal length between each alveolus (i.e., interalveolar spacing) tends to increase posteriorly (Table 2). Based on the photographs published by Kellner et al. (2013), the sizes of the alveoli are more variable in *Coloborhynchus clavirostris* than in *Ferrodraco* and the interalveolar spaces are shorter. The alveolar borders in *Ferrodraco* are more inflated relative to the jawline and are prominently scalloped. This combination of features unites *Ferrodraco* with *Mythunga*, although the condition observed in the latter taxon is even more pronounced than that in *Ferrodraco* (Molnar and Thulborn, 2007). By contrast, the alveolar borders in *Ferrodraco* are more prominent than those observed in *Tropeognathus mesembrinus* (Wellnhofer, 1987). Isolated teeth recovered during excavations (Figs. S5–8; Table S1), demonstrate that the degree of curvature as well as the variation in width differs in extent, such that *Ferrodraco* possesses a heterodont dentition. Based on the teeth and ironstone impressions on the lateral surfaces of the skull, the crown height of teeth occupying positions 1–4 does not exceed four times the tooth diameter. Moreover, the alveolar diameters of the first mandibular teeth suggest these teeth were not enlarged (Table 1). The first mandibular teeth are not separated by a thin sheet of bone as in the Targaryendraconia; rather, the width separating these teeth is subequal to the alveolar width. Although the total tooth count of the mandible cannot be determined based on the type specimen, it is interesting to note that in *Ferrodraco*, eight dentary alveoli are preserved anterior to the mandibular symphysis. By contrast, in *Tropeognathus mesembrinus* the eighth alveolus is level with the posterior margin of the mandibular symphysis (Wellnhofer, 1987), whereas 13 alveoli are situated anterior to the mandibular symphysis of "*Anhanguera robustus*" (Fig. S4H).

Frontal—The frontal is incomplete and triradiate in lateral view (Fig. 4A–F). The maximum anteroposterior length is 72 mm, whereas the dorsoventral height is 37 mm. This bone contributed to the dorsal margin of the orbit and forms part of the anterior and dorsal margins of the supratemporal fenestra. As this element is incomplete medially, it cannot be determined whether the frontals were fused along their midline. Although the frontal–postorbital contact is not preserved, the fact that the anterior portion tapers anteriorly means that it is likely that the anterior process was triangular, as in other anhanguerid pterosaurs. Unfortunately, the dorsal margin of the frontal is incomplete, such that the contact with the parietal is absent; therefore, the presence of a frontoparietal crest cannot be determined. As preserved, the frontal does not bear any striations, rugosities, or suture lines. The posterior portion of this element is incomplete, such that the shape of the dorsal margin of the supratemporal fenestra cannot be determined with certainty. Although the frontal is incomplete, the dorsal margin of the orbit is more ventrally positioned relative to the dorsal margin of the supratemporal fenestra. In this regard, the frontal of *Ferrodraco* is similar to that of *Anhanguera piscator* (Kellner and Tomida, 2000), but differs from that of *Anhanguera blittersdorffi* in which the dorsal margin of the orbit is situated more dorsally relative to the dorsal margin of the supratemporal fenestra (Pinheiro and Rodrigues, 2017). In some other anhanguerians, such as *Anhanguera spielbergi*, *Anhanguera* sp. (AMNH 22555), *Anhanguera* sp. (SNSB-BSPG 1987 I 47), and *Anhanguera* sp. (SAO 16494), the dorsal margins of the orbit and supratemporal fenestra appear approximately level (Pinheiro and Rodrigues, 2017; Veldmeijer, 2003; Wellnhofer, 1991a). Unfortunately, the lateral surface of the frontal is incomplete, and the contact between it and the postorbital is not preserved.

Surangular and Angular—The preserved portion of the surangular has a maximum length of 50 mm, a maximum dorsoventral height of 20 mm, and a maximum labiolingual width of 23 mm
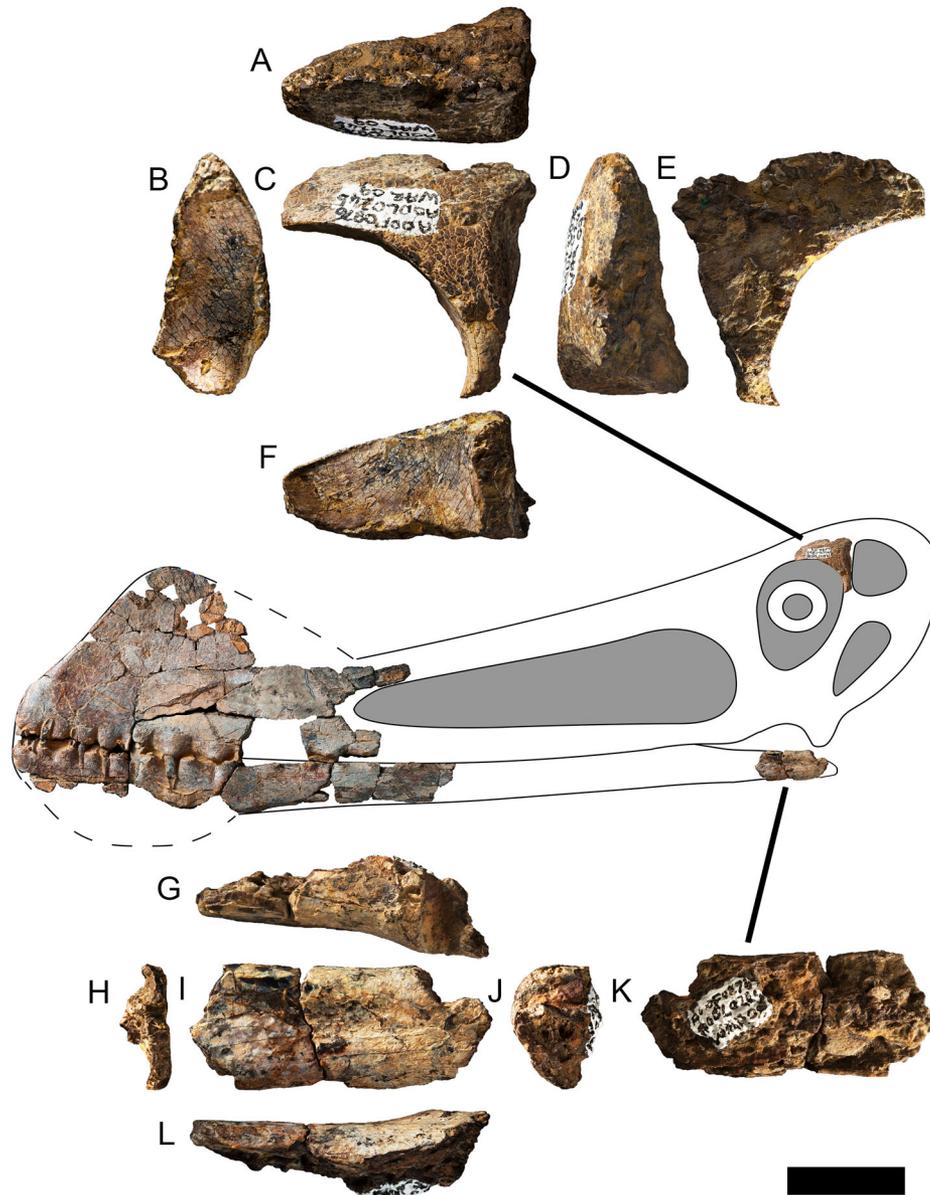
FIGURE 4. *Ferrodraco lentoni* holotype skull AODF 876 (modified from Pentland et al., 2019). **A–F**, left frontal in **A**, dorsal; **B**, anterior; **C**, lateral; **D**, posterior; **E**, medial; and **F**, ventral views. **G–L**, left mandibular articular region in **G**, dorsal; **H**, anterior; **I**, lateral; **J**, posterior; **K**, medial; and **L**, ventral views. All photographs taken by A.H.P. Scale bar equals 20 mm.

(Fig. 4G–L). Unfortunately, the retroarticular process in *Ferrodraco* is incomplete, such that the extent of the depressor fossa cannot be determined. Moreover, no pneumatic foramina were observed on the surangular/angular of *Ferrodraco*. The internal trabeculae observed on the retroarticular process in posterior view are comparatively large. By contrast, a large pneumatic foramen was observed on the retroarticular process, posteroventral to the medial cotyle by Wellnhofer (1991c) in *Anhanguera* sp. (AMNH 22555), and a similarly placed foramen in *Anhanguera spielbergi* by Veldmeijer (2003). The dorsal margin of this element is relatively flat, contrasting with that of *Aetodactylus* in which the dorsal margin is concave just anterior to the glenoid surface. In this respect, the dorsal margin of the surangular, angular, and articular is more similar to that of "*Anhanguera araripensis*" (SNSB-BSPG 1982 I 89; Wellnhofer, 1985) and *Anhanguera* sp. SNSB-BSPG 1987 I 47 (Wellnhofer, 1987).

Unfortunately, it cannot be determined whether the dorsal margin was relatively straight anteriorly, as in *Santanadactylus araripensis*, or if it was slightly raised dorsally, as in *Anhanguera* sp. (SAO 200602: Veldmeijer et al., 2005; AMNH 22555: Wellnhofer 1991c). The preserved portion of the glenoid in *Ferrodraco* is less prominent than that of *Aetodactylus* (Myers, 2010), but much larger than that of the indeterminate pterodactyloid UWPI 2349/101 (Buffetaut et al., 2011). In lateral view, the glenoid of *Ferrodraco* forms an angle of ca. 100°, unlike those of *Santanadactylus araripensis* and UWPI 2349/101, in which this angle is ca. 90° (Wellnhofer, 1985; Buffetaut et al., 2011). Based on the published schematic of *Anhanguera* sp. (AMNH 22555), the angle formed by the glenoid is even greater than that of *Ferrodraco* (Wellnhofer, 1991b; Pinheiro and Rodrigues, 2017). The glenoid surface of *Ferrodraco* also differs from *Anhanguera piscator* in that the retroarticular process is much

more inclined in the latter, such that the glenoid surface gently slopes (Kellner and Tomida, 2000).

Based on the synchrotron data, it could not be determined whether the angular and surangular are separate elements fossilized together, or if these elements had fused during ontogeny. Nevertheless, it is likely that the angular forms the ventrolateral-most surface of the mandibular ramus as in "*Anhanguera araripensis*" (SNSB-BSPG 1982 I 89) and "*Anhanguera santanae*" (BSP 1982 I 90; Wellnhofer, 1985). The dorsal surface of the lateral cotylus has been partially eroded; although its morphology cannot be determined with certainty, the exposed trabeculae on the dorsal surface are comparatively small. This would seem to suggest that little is missing from the dorsal surface. If this assumption is correct, the lateral cotylus of *Ferrodraco* is comparatively smaller and less extensive laterally than that in *Aetodactylus* (Myers, 2015). As this element is largely incomplete medially, the orientation of the medial cotylus cannot be determined.

Dentition—More than 40 teeth and tooth fragments of *Ferrodraco* were recovered, and although some of the corresponding alveoli have been identified, the majority remain disassociated (Figs. S5–8 and Table S1). In some isolated teeth, the pulp cavity was preserved (Fig. S5), whereas in other incomplete teeth this feature was not observed or greatly reduced (Fig. S7T). In some instances, crown–crown occlusion has resulted in the loss of the tooth apex (Figs. S5 and S6). Tooth wear was observed on teeth of varying size, and were typically gently inclined, relative to the long axis of the tooth. The isolated teeth also vary in size and curvature (Figs. S5–S8), with the largest isolated, near-complete tooth (AODF 876.T06) 30 mm in length, and the smallest (AODF 876.T31) only 10 mm in length (Table S1). Neither of these teeth are complete, with each lacking the tooth root. Based on these measurements, the longest tooth is three times longer than the shortest. By contrast, in *Zhenyuanopterus* the largest tooth was more than ten times the size of the smallest tooth (Lü, 2010). Although the teeth of *Ferrodraco* are somewhat variable, most are smooth and show very little ornamentation. However, impressions of maxillary teeth preserved in ironstone on the mandible bear fine longitudinal striations. This seems to suggest that striations were more common in the dentition of *Ferrodraco* and removed either during fossilization or after fossilization but prior to collection. Alternatively, striations may be localized within the anterior section of the jaws, and teeth located posteriorly may be smooth and unornamented. Wang et al. (2012) also noted that the teeth of *Guidraco* were mostly smooth, with some striations observed near the roots on the lingual surface. Based on this observation, it is also highly likely that striations are worn unevenly, such that they are effectively lost in areas of more extensive contact, i.e., near the tooth apex. *Guidraco* differs from *Ferrodraco* in that the anterior teeth are inclined and extremely elongate, such that their apices surpass the margin of the maxilla during occlusion (Wang et al., 2012).

Cervical Vertebrae

The vertebral column of *Ferrodraco* is represented by five partial cervical vertebrae (Fig. 5). Owing to the fragmentary nature of these vertebrae, their precise positions within the vertebral column cannot be determined. The anteriormost cervical vertebra of determinate position is referred to here as cervical vertebra A, the second anteriormost vertebra as cervical vertebra B and so on. All other vertebrae are regarded based on the completeness of each element (i.e., the least complete vertebra of indeterminate position within the cervical series is referred to last). All vertebrae for which the condyle and cotyle are preserved are procoelous, as in other pterosaurs. As noted in other pterosaur cervical vertebrae these elements are hollow;

however, the cervical vertebrae of *Ferrodraco* are three-dimensionally preserved owing to ironstone infill.

Cervical vertebra A (WAR15) is represented by a partial centrum comprising a condyle and the right exapophysis (Fig. 5A–F). The dorsal, anterior, and left lateral surfaces are incomplete, revealing the internal trabeculae infilled with matrix. As preserved, it is 21 mm anteroposteriorly, the centrum is 11 mm dorsoventrally (excluding the exapophysis) and 21 mm laterally, including the exapophysis. The condyle and exapophysis preserved in this vertebra appear laterally wider and more robust when compared with those of cervical vertebra B. Based on comparisons with the cervical vertebra of *Anhanguera* sp. (AMNH 22555; Wellnhofer, 1991c), cervical vertebra A is tentatively identified as cervical vertebra IV, based on the angle between the exapophysis and condyle.

Cervical vertebra B (WAR14) is the most complete of those recovered and preserves the condyle, cotyle, floor of the neural canal, most of the right postexapophysis and part of the left exapophysis (Fig. 5G–L). The neural spine, prezygapophyses, and postzygapophyses were evidently lost prior to collection. As preserved, cervical vertebra B is 27 mm in length, 18 mm across at its widest point and 18 mm dorsoventrally. A large oval pneumatic foramen is present on the right lateral surface, whereas the neural canal is visible dorsally as a longitudinal groove. The concave anterior cotyle is subcircular in outline and still partially obscured by matrix. Based on the angle of the exapophysis relative to the condyle, and the relative dimensions of the centrum, it is tentatively identified here as cervical vertebra VII, based on comparisons with *Anhanguera* sp. (AMNH 22555; Wellnhofer, 1991c).

Cervical vertebra C (WAR12) comprises a partial centrum and preserves the remnants of the prezygapophyses and postzygapophyses (Fig. 5M–R). Large oval pneumatic foramina were observed on both the left and right lateral surfaces. The dorsal surface of this vertebra is incomplete and is still partially obscured by matrix. The anterior and posterior surfaces are both incomplete. As preserved, the vertebra is 28 mm in length, 9 mm in height dorsoventrally, 19 mm across as measured at the prezygapophyses and 16 mm across at the postzygapophyses.

Cervical vertebra D, comprising a partial centrum, is less complete than cervical vertebra C and comprises an incomplete condyle (Fig. 5S–X). The dorsal, anterior and left lateral surfaces are incomplete, with the right lateral surface slightly better preserved than the left. As preserved this centrum is 16 mm anteroposteriorly, 7 mm dorsoventrally and 15 mm transversely, measured at its widest point. No lateral pneumatic foramina were identified. The internal bone exposed on the dorsal surface is infilled with matrix and gypsum.

Cervical vertebra E comprises a partial centrum, including a small portion of the exapophysis, and is 18 mm anteroposteriorly, 10 mm dorsoventrally and 12 mm transversely at its widest point (Fig. 5Y–AD). The left lateral surface preserves cortical bone whereas the other surfaces are incomplete and the dorsal surface is partially obscured by ironstone. Compared with the other cervical vertebra, this element is morphologically uninformative. Attempts to join cervical vertebra E with other cervical vertebrae have proven unsuccessful.

Scapulocoracoid

The pectoral girdle is only represented by an incomplete right scapulocoracoid (Fig. 6A–F). This in turn is represented by part of the glenoid, comprising the articular surface, supraglenoidal buttress and lower tubercle. Although the supraglenoidal buttress and lower tubercle are incomplete, with small sized trabeculae preserved, the supraglenoidal buttress appears to have projected further ventrally than the lower
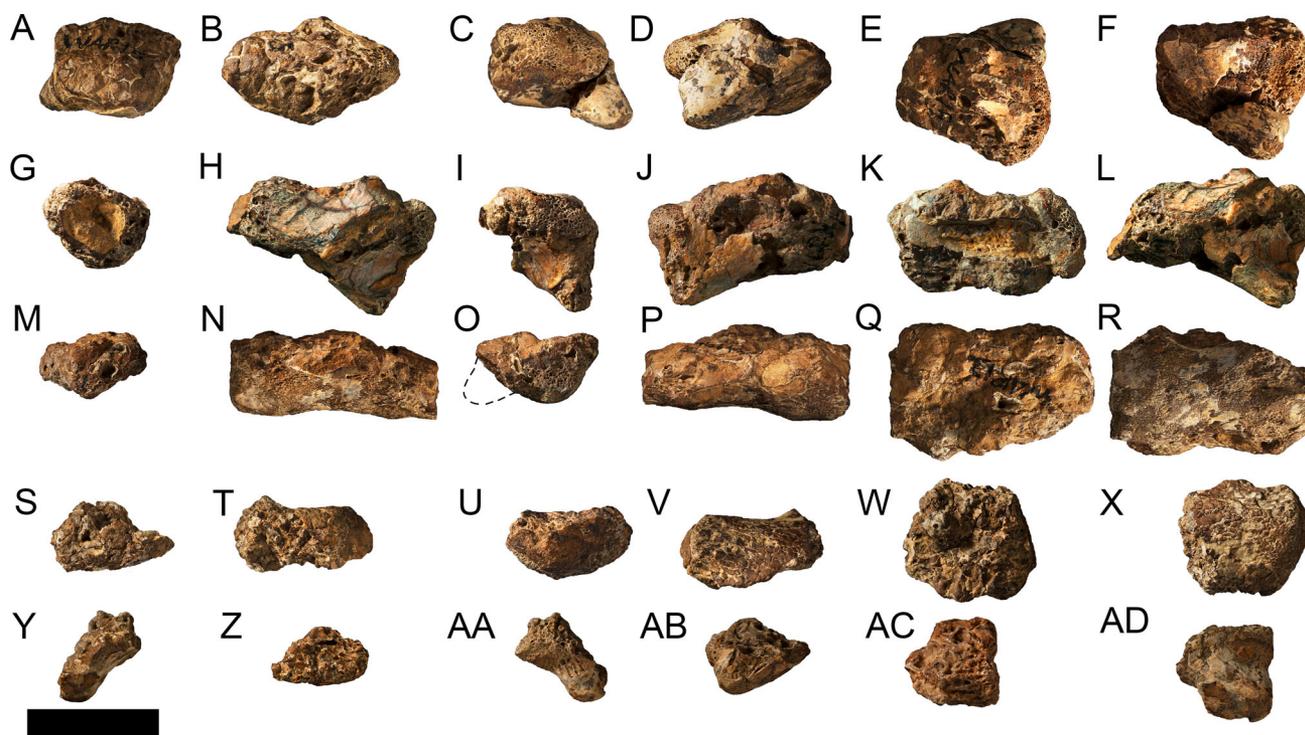
FIGURE 5. *Ferrodraco lentoni* holotype cervical vertebrae AODF 876. **A–F**, cervical vertebra A in **A**, anterior; **B**, left lateral; **C**, posterior; **D**, right lateral; **E**, dorsal; and **F**, ventral views. **G–L**, cervical vertebra B in **G**, anterior; **H**, left lateral; **I**, posterior; **J**, right lateral; **K**, dorsal; and **L**, ventral views. **M–R**, cervical vertebra C in **M**, anterior; **N**, left lateral; **O**, posterior; **P**, right lateral; **Q**, dorsal; and **R**, ventral views. **S–X**, cervical vertebra D in **S**, anterior; **T**, left lateral; **U**, posterior; **V**, right lateral; **W**, dorsal; and **X**, ventral views. **Y–AD**, cervical vertebra E in **Y**, anterior; **Z**, left lateral; **AA**, posterior; **AB**, right lateral; **AC**, dorsal; and **AD**, ventral views. The dashed line represents the missing portion of the extent of the missing exapophysis. All photographs taken by A.H.P. Scale bar equals 20 mm.

tubercle. Despite the fact that the scapulocoracoid is largely incomplete, fusion of this element indicates that the type individual of *Ferrodraco lentoni* was ontogenetically mature. The suture between these elements is less prominent when compared with *Anhanguera* sp. (AMNH 22555; Wellnhofer 1991c). In this regard, its condition is similar to that observed in *Anhanguera spielbergi* (Veldmeijer, 2003). By contrast, Kellner and Tomida (2000) noted that these elements are unfused in *Anhanguera piscator*, although they are preserved together. The scapulocoracoid is incomplete proximally, such that a process on the scapula cannot be determined. Similarly, based on the preserved portion of the coracoid, it is unclear as to whether a process was present on the anterior surface of the coracoid as in *Anhanguera piscator* (Kellner and Tomida, 2000) or *Anhanguera* sp. (AMNH 22555; Wellnhofer, 1991c). The lateral surface of the glenoid is three-dimensionally preserved; however, the posterior margin has been eroded, revealing the internal trabeculae. By contrast, the posterior surface is crushed and distorted, resulting in anteroposterior flattening of the preserved portion of the coracoid shaft. The preserved portion of the coracoid shaft is 18 mm wide. No pneumatic foramina or grooves were identified in this specimen; however, the scapulocoracoid does appear somewhat crushed and distorted. Although the articular surface of the scapula is incomplete, the supraglenoidal buttress projects further ventrally than *Anhanguera piscator* (Kellner and Tomida, 2000). Moreover, the lower tubercle is more pronounced than in *Anhanguera piscator* (Kellner and Tomida, 2000) and *Anhanguera spielbergi* (Veldmeijer, 2003), with the ventral margin of the glenoid fossa sloping anteriorly at an angle of ca. 90 degrees.

Ulna

As preserved, the left ulna comprises part of the diaphysis and the distal end, with the shaft anteroposteriorly compressed and the distal articular surface dorsoventrally expanded (Fig. 6G–L). The distal articular surface is 57 mm dorsoventrally and 19 mm anteroposteriorly. Much of the bone is an ironstone cast, with some distortion to the posterior surface of the shaft. This damaged section of the shaft is incomplete and associated with gypsum crystals. Despite incomplete preservation, the ulna preserves cortical bone ca. 1 mm thick on the distal end and part of the anterior surface of the shaft. Given that the proximal end of the diaphysis is slightly expanded, it is unlikely that more than half of the total length of the ulna is missing. If correct, then the total length of the ulna is subequal to, or less than double, the length of metacarpal IV, as in lanceodontian pterosaurs generally (Wellnhofer, 1991c; Kellner and Tomida, 2000; Lü, 2010; Elgin and Frey, 2011). In posterior view, the dorsal margin is concave whereas the ventral margin is relatively straight. The anterior surface of the ulna shaft is flat and preserves ironstone as well as cortical bone from the radius on the ventral margin. No pneumatic foramen was observed on the anterior surface. The ventral crest in the present specimen is more strongly developed than in MACN-SC 3617 (Kellner et al., 2003), slightly ventrally expanded, but less projected when compared with *Santanadactylus araripensis* (BSP 1982 I 89; Wellnhofer, 1985). In terms of its morphology, the ventral crest on the distal articulation in *Ferrodraco* is similar to that of *Santanadactylus araripensis* (BSP 1982 I 89; Wellnhofer, 1985), in that the margin is straight and ventrally sloping. The ventral fovea carpalis located on the distal articular surface is
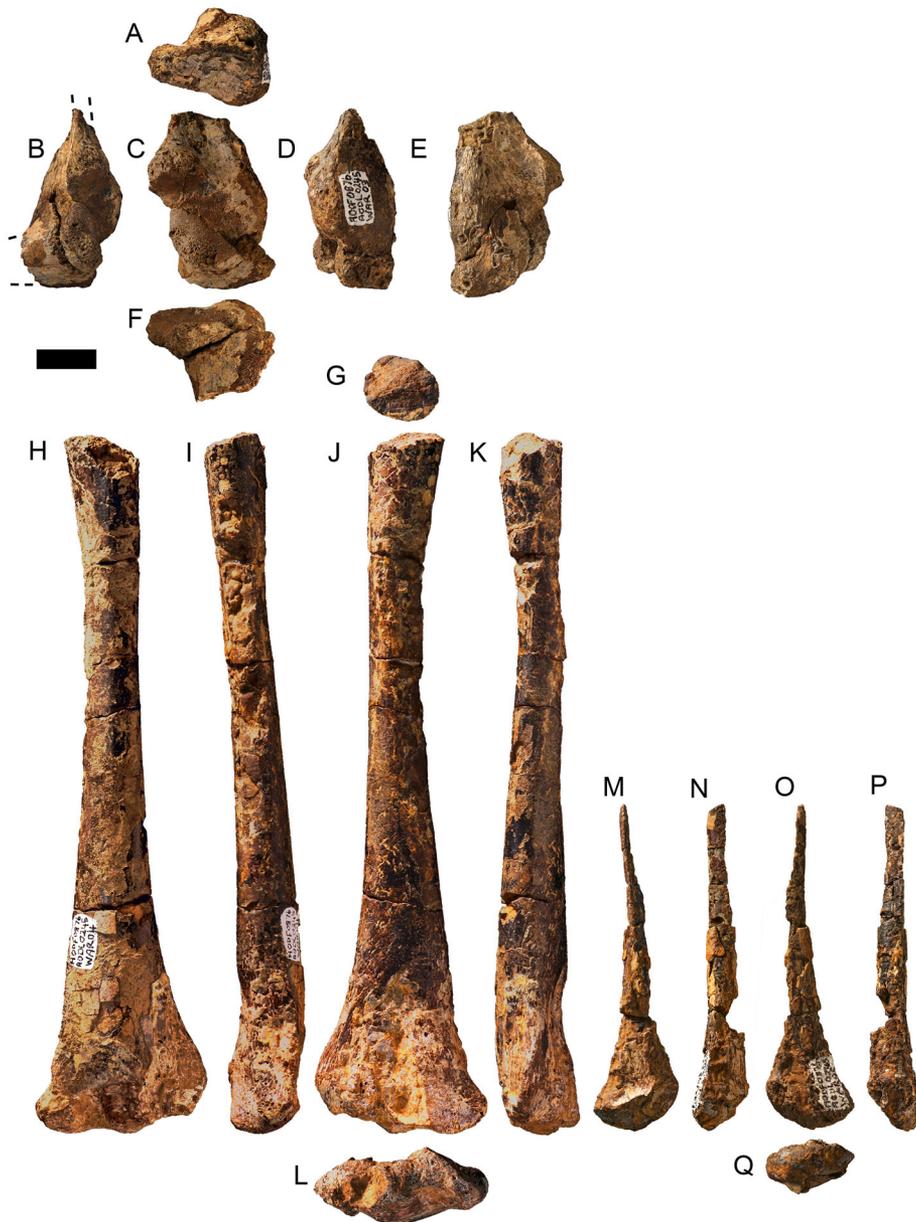
FIGURE 6. *Ferrodraco lentoni* holotype appendicular elements AODF 876. **A–F**, right scapulocoracoid in **A**, dorsal; **B**, posterior; **C**, lateral; **D**, anterior; **E**, medial; and **F**, ventral views. **G–L**, left ulna in **G**, proximal; **H**, posterior; **I**, lateral; **J**, anterior; **K**, medial; and **L**, distal views. **M–Q**, left radius in **M**, posterior; **N**, lateral; **O**, anterior; **P**, medial; and **Q**, distal views. All photographs taken by A.H.P. Scale bar equals 20 mm.

ca. 6 mm in diameter. As in other anhanguerid pterosaurs, the distal articular surface of *Ferrodraco* bears a ventral ridge.

Radius

The left radius is incomplete and only preserves the distal end and a crushed portion of the diaphysis (Fig. 6M–Q). Although the diaphysis has been dorsoventrally crushed and only preserves cortical bone in some places, the distal end is three-dimensionally preserved and interpreted here as representative of its true morphology. The articular surface is convex with a distinct depression located on the dorsal margin. The anterior surface of the radius shaft preserves the impression of the left ulna and its cortical bone, based on synchrotron data, indicating the radius and ulna were articulated during fossilization. The point at which the radius receives the ulna has been left unprepared; as such, the nature of the contact against the ulna cannot be determined. The proximal portion of the radius shaft has been crushed such that it appears semi-circular in cross-section, with the flat surface on the dorsal margin. Owing to taphonomic crushing, the original shape of the shaft cross-section cannot be determined. At its break, the proximal portion of the radius shaft is 5 mm anteroposteriorly. The external bone on the posterior surface of the shaft has been eroded, revealing the internal trabeculae, with the ventral portion of the posterior surface more eroded than the dorsal portion. Given that the posterior surface has been eroded, it is possible that the distal aspect of the radius has been somewhat distorted; however, this is not unequivocally supported herein. In distal aspect the radius in *Ferrodraco* is similar to that of *Santanadactylus araripensis* (SNSB-
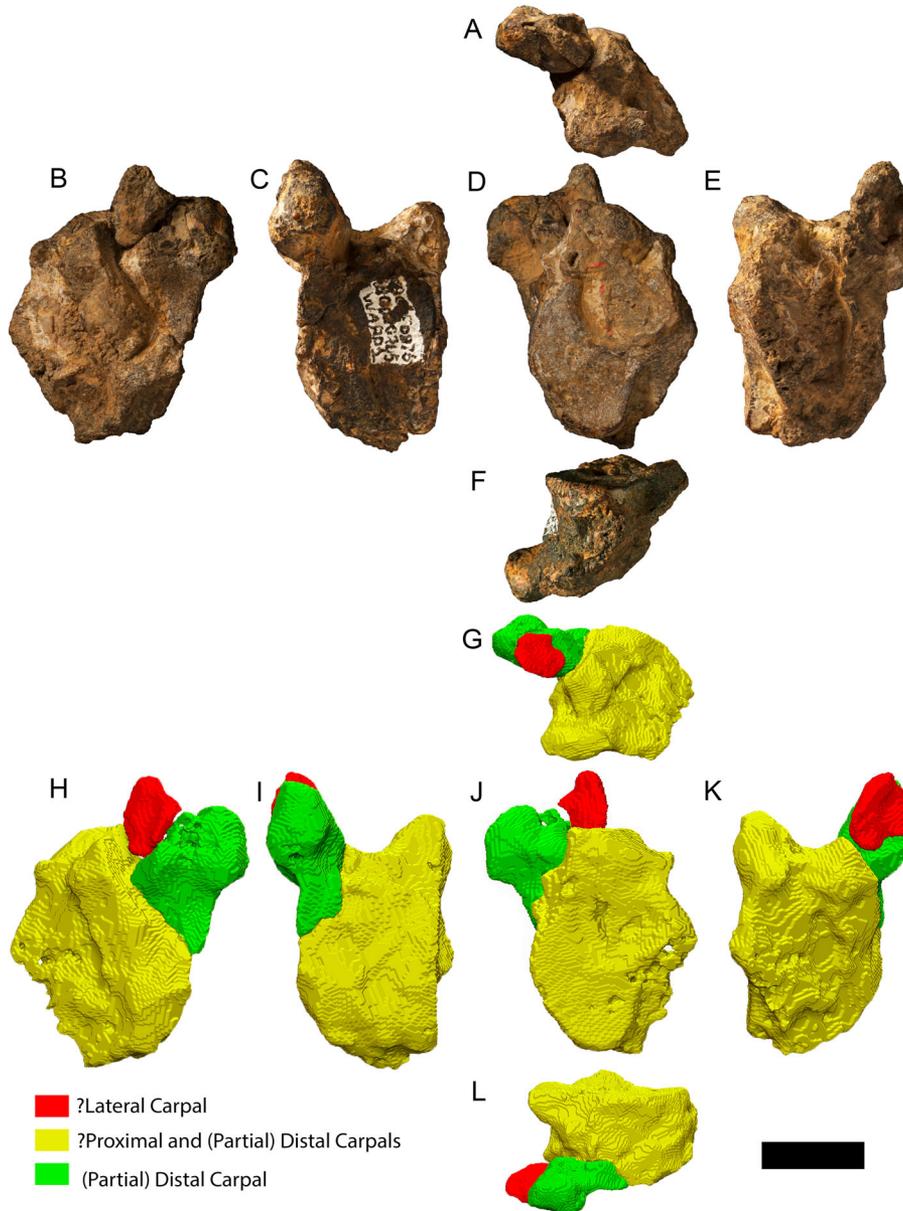
FIGURE 7. *Ferrodraco lentoni* holotype left syncarpus AODF 876. **A–F**, photographs of the left syncarpus in **A**, anterior; **B**, proximal; **C**, ventral; **D**, distal; **E**, dorsal; and **F**, posterior views. **G–L**, three-dimensional surface renders based on CT scan data of syncarpus in **G**, anterior; **H**, proximal; **I**, ventral; **J**, distal; **K**, dorsal; and **L**, posterior views. All photographs taken by A.H.P., 3D renders by M.A.W. Scale bar equals 20 mm.

BSPG 1982 I 89; Wellnhofer, 1985) and *Anhanguera* sp. (AMNH 22555; Wellnhofer, 1991c) but is more elongate dorsoventrally and bears a posterior ridge.

Syncarpus

The left carpus (Fig. 7A–L) comprises the proximal and distal carpals preserved together, but not fused (Fig. 7G–L). Moreover, pneumatic foramina were not observed on the dorsal or ventral surfaces. The distal and proximal articular surfaces of the carpus are subequal in size and well-preserved; however, the proximal articular surface is still partially obscured by matrix. The proximal articular surface is pentagonal in outline and

bears a rounded ridge on its dorsal margin. A more prominent rectangular ridge is located on the dorsal margin, and is ca. 9 mm wide and 23 mm in length. Overall, the morphology of the proximal articular surface compares favorably with *Anhanguera* sp. (AMNH 22555) in terms of the morphology of the articular surfaces that receive the ulna and radius (Wellnhofer, 1991c). Medially, the proximal articular surface is concave; however, no pneumatic foramen was identified. The distal articular surface of the carpus corresponds well with the proximal articular surface of metacarpal IV; however, given that the proximal portion of the left metacarpal differs from that of the right metacarpal, the morphology of this surface is interpreted with caution. Nevertheless, the distal articular surface is
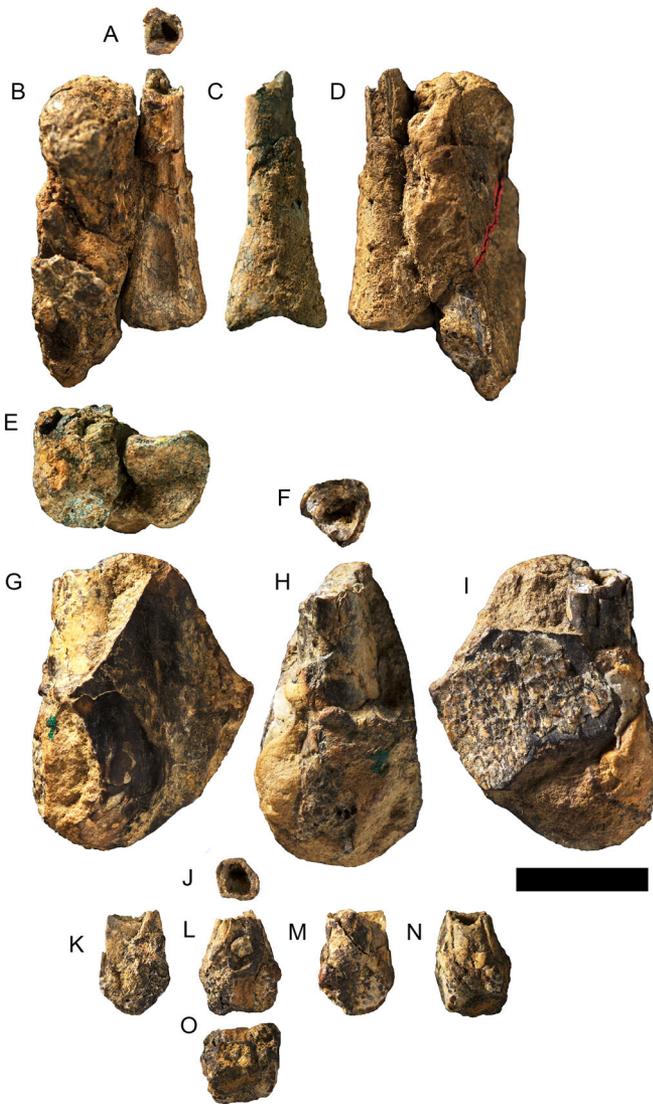
FIGURE 8. *Ferrodraco lentoni* holotype indeterminate non-wing manual phalanges AODF 876. **A–E**, left non-wing manual phalanx A in **A**, distal; **B**, anterior; **C**, lateral; **D**, posterior; and **E**, proximal views. **F–I**, left non-flight digit metacarpal B in **F**, ? proximal; **G**, ?anterior; **H**, lateral; and **I**, ? posterior views. **J–O**, left non-wing manual phalanx C in **J**, proximal; **K**, medial; **L**, posterior; **M**, lateral; **N**, anterior; and **O**, distal views. All photographs taken by A.H.P. Scale bar equals 10 mm.

triangular in outline, with the anterior margin more expanded than the posterior margin. Only the posterior portion has been fully prepared and is concave and crescentic with the tips of the crescent pointing anterodorsally and anteriorly (Fig. 7D). The anterior portion of the distal articular surface is unprepared; however, it is clearly smaller when compared with the posterior portion, which is corroborated by CT scan data (Fig. 7J). Although there is a medially located groove on the distal articular surface, a pneumatic foramen was not observed. During analysis of CT scan data (Fig. 7G–L), an additional element (red) was identified in association with the proximal (yellow) and distal carpals (green). Based on comparisons with *Anhanguera* sp. (AMNH 22555; Wellnhofer, 1991c) this element is tentatively identified here as part of the lateral carpal (contra Pentland et al., 2019). Unfortunately, little more can be ascertained regarding its morphology.

Phalanges I–III

During excavations, three incomplete phalanges were recovered (Fig. 8A–O); however, none of the preserved elements can be precisely attributed to phalanx I, II, or III. Owing to incomplete preservation, it cannot be determined whether the phalanges reached the distal syncarpal nor the position of their distal ends relative to one another. No manual unguals were recovered during excavation.

The distal end of one of the manual phalanges, now embedded in ironstone (Fig. 8F–I), fits the medial groove of the left metacarpal IV and distally abuts the condyles, indicating these bones were articulated during fossilization. Another fragment associated with matrix (Fig. 8A–E) preserves the proximal end of another phalanx: the shaft is narrow, bears a groove located on the anterior surface and is crescentic in transverse cross-section such that the concave margin is on the anterior surface. Although the distal end of a phalanx was also recovered (Fig. 8J–O), attempts to join it with the proximal end of a phalanx have proven unsuccessful. The proximal articular surface is triangular in outline, convex and anteroposteriorly expanded.

Metacarpal IV

Both the left and right metacarpal IV are preserved (Fig. 9A–K). The right metacarpal IV is incomplete and comprises the proximal articular surface and part of the diaphysis. Although largely undistorted, the distal end of the shaft has been anteroposteriorly flattened, and parts of the posterior surface are incomplete, such that the internal trabeculae are exposed with associated gypsum crystals.

The left metacarpal IV is complete, but has been anteroposteriorly flattened (Fig. 9F–K). Based on comparisons with the incomplete right metacarpal IV (Fig. 9A–E), the proximal end of the left metacarpal IV has suffered some distortion. However, the distal end remains three-dimensionally preserved and articulates with the extensor tendon process fused to the proximal end of the first wing phalanx. The distal articular surface is 29 mm anteroposteriorly, whereas dorsoventrally, the major tubercle is 34 mm, the minor tubercle is 24 mm and the midpoint between these tubercles is 21 mm. Unfortunately, the anterior surface of the shaft is damaged, such that the presence of a pneumatic foramen near the distal end cannot be determined. In posterior view, the shaft of the left metacarpal is concave towards the midline. Nevertheless, ironstone preserved on the proximal end of the left metacarpal corresponds to the ironstone preserved on the left distal syncarpal, indicating these elements were articulated during fossilization.

First Wing Phalanx

The left first wing phalanx is incomplete and is represented by the proximal end and most of the shaft (Fig. 9L–P), as well as part of the distal end. The proximal articular surface is almost complete, however the ventral margin of the dorsal fossa is missing and the anterior portion of the extensor tendon process is slightly eroded on its posterior margin. The ventral fossa is complete but partially obscured by ironstone. The maximum width of the proximal articular surface is 54 mm anteroposteriorly. By contrast, the maximum width of the proximal articular surface of *Anhanguera piscator* was reported as 65 mm by Kellner and Tomida (2000), who noted its size was comparable to that of *Araripedactylus dehmi* (BSP 1975 I 166). As preserved, the first wing phalanx of *Ferrodraco* is relatively straight, 310 mm in length and the transverse cross-section of the shaft is subtriangular. The ventral margin of the first wing phalanx is crushed. Cortical bone is

FIGURE 9. *Ferrodraco lentoni* holotype flight digit metacarpals and phalanges AODF 876. **A–E**, right metacarpal IV in **A**, proximal; **B**, ventral; **C**, anterior; **D**, dorsal; and **E**, posterior views. **F–K**, left metacarpal IV in **F**, proximal; **G**, dorsal; **H**, anterior; **I**, ventral; **J**, posterior; and **K**, distal views. **L–P**, proximal end of left first wing phalanx (IV-1) in **L**, proximal; **M**, posterior; **N**, dorsal; **O**, anterior; and **P**, ventral views. **Q–U**, distal end of left first wing phalanx in **Q**, posterior; **R**, dorsal; **S**, anterior; **T**, ventral; and **U**, distal views. The dashed line represents the missing portion of the diaphysis. All photographs taken by A.H.P. Scale bar equals 50 mm.

preserved along the anterior margin of the shaft, near the distal end on the ventral margin and the proximal articular surface. Unfortunately, much of the ventral margin of the shaft is crushed and the cortical bone is missing. As such, it cannot be determined whether the ventral margin of the shaft had a rugose texture, as reported in *Anhanguera piscator* by Kellner and Tomida (2000). Although the distal portion of the shaft is heavily crushed, it is clear that it is not transversely expanded.

As in other anhanguerid pterosaurs, the extensor tendon process has an anteroposteriorly expanded base, with two projections; the largest is vertically oriented and the smaller of the two projects anteriorly. Given that the tip of the extensor tendon process is irregular and less robust when compared with *Anhanguera piscator*, it is likely that a small section of the extensor tendon process is missing. Moreover, the extensor tendon process is weaker and less posteriorly deflected when compared with *Santanadactylus pricei* (AMNH 22552; Wellnhofer 1991c). The slope of the posterior margin of the extensor tendon process in *Ferrodraco* is defined by a sharp ridge that is similar to *Anhanguera piscator* (Kellner and Tomida, 2000); however, the slope of this ridge is gentler when compared with that of *Santanadactylus pricei* (AMNH 22552; Wellnhofer 1991c). The anterior margin of the extensor tendon process appears less constricted than that of *Anhanguera piscator*. Given that the extensor tendon process in *Anhanguera piscator*

is unfused (Kellner and Tomida, 2000), it is not unexpected that its morphology differs from the extensor tendon process in the present specimen.

The distal end of the left first wing phalanx was also recovered during excavations (Fig. 9Q–U). This element has a triangular outline when observed in distal view, such that the complete surface represents the posterior surface. The posterior surface is defined by a ridge, as in *Santanadactylus pricei* (Wellnhofer, 1985). Unfortunately, the anterior surface does not preserve the internal trabeculae and no pneumatic foramina were observed.

DISCUSSION

The Phylogenetic Affinities of Australian Pterosaur Taxa

Ferrodraco was initially resolved as the sister taxon to *Mythunga camara*, with both assigned to the Ornithocheirinae (Pentland et al., 2019). More recently, the phylogenetic positions of *Ferrodraco* and *Mythunga* were reassessed by Holgado and Pêgas (2020). These authors utilized a modified version of the dataset employed by Pêgas et al. (2019), with inclusion of characters from Jacobs et al. (2019), and the addition of new taxa and characters pertaining to the rostrum. Holgado and Pêgas (2020) also recognized *Ferrodraco* and *Mythunga* as sister taxa. However, *Tropeognathus mesembrinus* + *Siroccopteryx moroccensis* were resolved as the sister taxon to this clade, with all four taxa grouped together in the new clade Tropeognathinae. By contrast, *Ornithocheirus simus* was considered as the sister taxon to the clade *Ferrodraco* + *Mythunga* by Pentland et al. (2019).

Although Holgado and Pêgas (2020) scored *Ferrodraco* for 73 of the 179 discrete characters (40.8%), these scores pertain to cranial and dental characters only. Here we present an updated version of the data matrix presented by Holgado and Pêgas (2020), for which *Ferrodraco* can be assessed for 83 of the 179 character states. Bremer supports vary from 1 to 3 throughout the tree, with most nodes poorly supported.

The results of both analyses support the close relationship between *Ferrodraco lentoni* and *Mythunga camara* (Fig. 10). We support the interpretation made by Holgado and Pêgas (2020) that together they form a clade (as noted in Pentland et al. [2019] and Fig. 10A) that lies outside Anhanguerinae. However, the precise position of these two taxa remains uncertain: although they have been included within Tropeognathinae (Fig. 10A), as in Holgado and Pêgas (2020), in the absence of this clade, they are placed in Coloborhynchinae in a polytomy with *Tropeognathus* (Fig. 10B). These results contrast with those of Pentland et al. (2019), in which *Ferrodraco* and *Mythunga* were more closely related to *Ornithocheirus simus*, a result that suggested ornithocheirids were cosmopolitan during the Early–mid-Cretaceous. By contrast, the phylogenetic analyses presented here (Fig. S9), combined with those of Holgado and Pêgas (2020) in which *Ferrodraco* + *Mythunga* were considered sister taxa to *Tropeognathus* + *Siroccopteryx*, suggest that the subfamily Tropeognathinae was restricted to Gondwana, in agreement with Holgado and Pêgas (2020). Indeed, the topology of Fig. 10A is the same as that of Holgado and Pêgas (2020), with the exception of the Targaryendraconia. In both analyses, the clade Targaryendraconia is supported; however, in the first analysis (Fig. 10A), *Targaryendraco wiedenrothi*, *Aussiedraco molnari*, *Barbosania gracilirostris*, *Cimoliopterus cuvieri*, *Cimoliopterus dunni*, *Aetodactylus halli*, and *Camposipterus nasutus* were resolved in a polytomy, with no support for Targaryendraconidae. By contrast, the Targaryendraconidae was resolved in the second analysis (Fig. 10B), which was based on a modified version of the Pêgas et al. (2019) dataset. Given that many members of the Targaryendraconia are known only from incomplete cranial specimens, more complete and better-

preserved material will be needed to establish the interrelationships within this clade.

Comparisons with *Ferrodraco* and Other Australian Pterosaur Material

Although its precise position within Anhangueridae remains uncertain (see Holgado and Pêgas, 2020; Pentland et al., 2019), it is clear that *Ferrodraco* belongs in this clade. As the majority of the isolated pterosaur remains reported from Australia have been interpreted as ornithocheirids sensu Unwin (2003), comparisons with *Ferrodraco* in instances where material overlaps might provide additional information on their taxonomic affinities. However, it is worth noting that although the Australian pterosaur fauna is dominated by ornithocheirids, exceptions include a ctenochasmatoid humerus from the upper Albian Mackunda Formation (Fletcher and Salisbury, 2010) and an azhdarchid ulna from the Maastrichtian Miria Formation (Bennett and Long, 1991). Although several members of the Targaryendraconia and Tropeognathinae are known only from incomplete cranial material, comparisons with *Ferrodraco* and several Australian pterosaurs, as well as revised descriptions of the latter, are suggestive of greater diversity in the Australian pterosaur fauna.

Aside from *Mythunga camara* (Molnar and Thulborn, 2007), *Aussiedraco molnari* (Fig. 11A–E; Kellner et al., 2011) and the recently described *Thapunngaka shawi* (Richards et al., 2021), there are two other fragmentary pterosaur crania known from Australia with which *Ferrodraco lentoni* can be compared: QM F44423 and WAM 68.5.11. The geologically older of the two is a partial mandibular rostrum, QM F44423 (Fig. 11F–I), recovered east of Hughenden (Hughenden–Redcliffe Road, NE of Mt. Walker), in rocks of the upper Albian Toolebuc Formation. QM F44423 was first illustrated and described by Fletcher and Salisbury (2010) and assigned to an indeterminate genus of ornithocheirid (sensu Unwin 2001). The rostral end of QM F44423 is near-complete, comprising a portion of the mandibular rostrum and preserving left alveoli 1–8 and right alveoli 1–7 (Fletcher and Salisbury, 2010). QM F44423 does not preserve a mandibular symphysis, but the posterior segment is laterally expanded with respect to the anterior part portion of the rostrum.

QM F44423 differs from other members of the Ornithocheiridae in that there seems to be little variation along the tooth row, based on the preserved alveolar diameter (Fletcher and Salisbury, 2010:table 1). The specimen also lacks the terminal expansion of the mandible and sagittal crest; however, crests are absent in several ornithocheirids, including *Brasileodactylus*, *Boreopterus*, and *Ludodactylus sibbicki*, and this might be a sexually dimorphic character (Fletcher and Salisbury, 2010; Hone et al., 2012). Given that the ontogenetic status of QM F44423 cannot be determined, and in the absence of more complete material, it would be premature to rule out the possibility that this specimen represents an immature individual.

Recently, QM F44423 was compared with *Targaryendraco* and *Aussiedraco* (Pêgas et al., 2019). As noted by Pêgas et al. (2019), the jawline in QM F44423 is scalloped because of the inflation of the alveolar borders; however, the degree of inflation is less exaggerated when compared with *Mythunga* and *Ferrodraco*. QM F44423 differs from targaryendraconians in that the first tooth pair is vertical, the third tooth pair is not enlarged relative to other mandibular teeth, and the mandibular groove becomes transversely wider posteriorly (Pêgas et al., 2019). The latter differs from the condition in targaryendraconians (Pêgas et al., 2019), and in this regard, QM F44423 is more similar to *Ferrodraco* and *Tropeognathus mesembrinus*. However, QM F44423 differs from *Ferrodraco* and *Tropeognathus*, in that it lacks a mandibular crest (Fletcher and
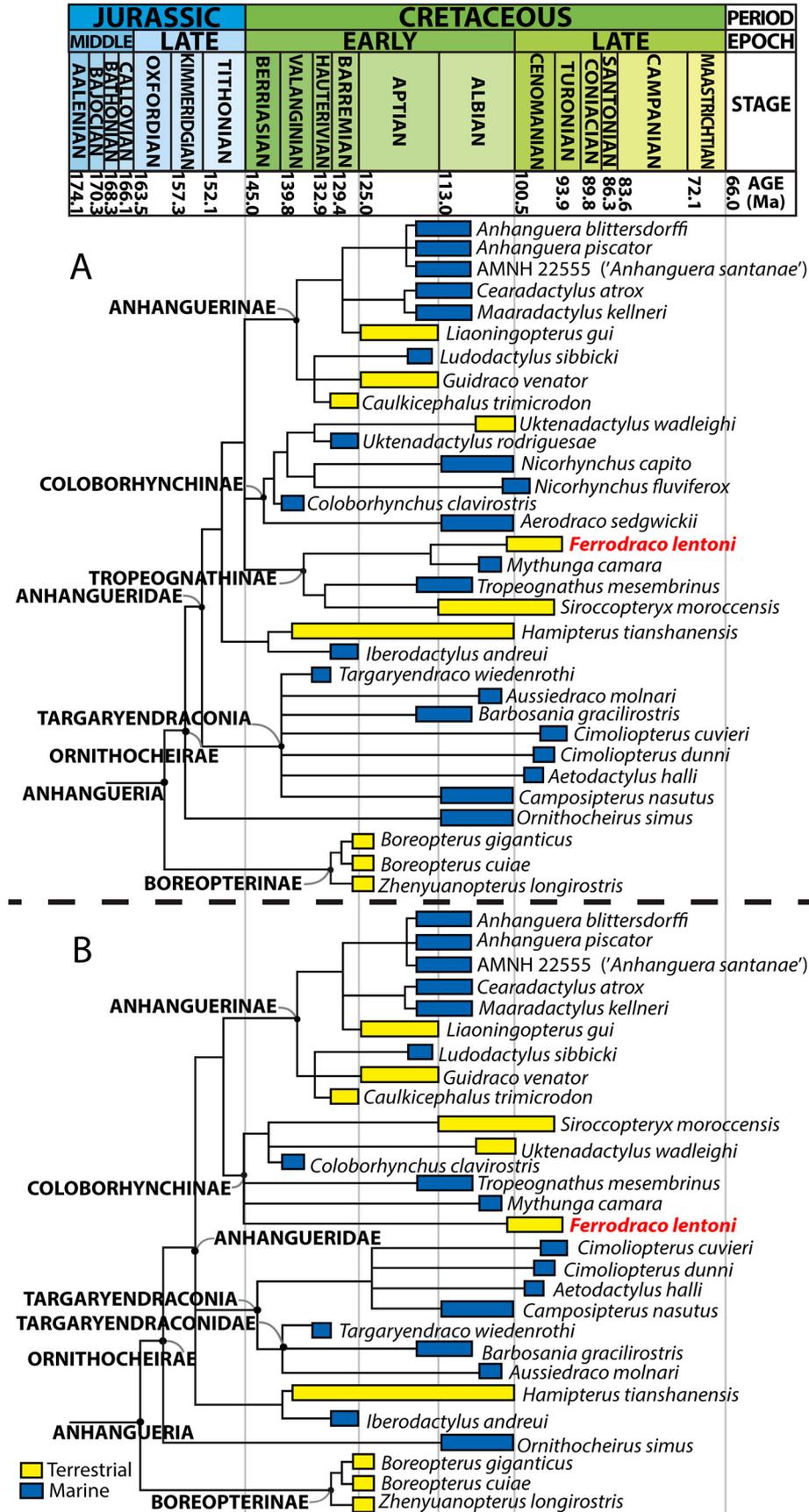
FIGURE 10. Time-calibrated phylogenetic trees of Anhangueria. The box next to each taxon denotes its temporal range (including stratigraphic uncertainty). **A**, tree based on the matrix of Holgado and Pêgas (2020); **B**, tree based on the matrix of Pêgas et al. (2019), with *Ferrodraco lentoni* and *Mythunga camara* included. Figure drafted by A.H.P.

FIGURE 11. Partial pterosaur dentaries derived from the upper Albian Toolebuc Formation. **A–E**, *Aussiedraco molnari* holotype QM F10613 in **A**, dorsal, **B**, anterior, **C**, right lateral, **D**, left lateral, and **E**, ventral views. **F–I**, partial mandible, QM F44423 in **F**, left lateral, **G**, dorsal, **H**, right lateral, and **I**, ventral views. All photographs taken by S.F.P. Scale bar equals 10 mm.

Salisbury, 2010) and is transversely narrower. Although the mandibular groove is flanked by ridges on either side, these are not tall as in the Targaryendraconia. Given that a mandibular groove can only be observed with certainty as far as the posterior margin of the fourth alveoli in *Aussiedraco*, it cannot be determined whether it widens posteriorly, as in QM F44423.

The most obvious difference between *Ferrodraco* and QM F44423 is the presence of a mandibular crest in the former. Moreover, the dorsoventral height of the mandibular symphysis of *Ferrodraco* excluding the fragmentary crest exceeds that of QM F44423. *Ferrodraco* and QM F44423 are similar, in that the lateral width of the mandibular symphysis is over three times the alveolar diameter in both. However, they differ in that the

mandibular groove in *Ferrodraco* initiates posterior to the second pair of alveoli, whereas this feature initiates anterior to the first pair of alveoli in QM F44423. QM F44423 also differs from *Ferrodraco*, in that the mandibular groove is more pronounced and transversely expanded posteriorly in the latter. Although the QM F44423 mandible is incomplete, it is clear that the mandibular groove extends posterior to the eighth pair of alveoli. Therefore, it cannot be determined whether the mandibular groove terminates at the posterior margin of the mandibular symphysis, as in *Ferrodraco* and *Tropeognathus mesembrinus* (Wellnhofer, 1987; Fig. 2). In both *Ferrodraco* and *Tropeognathus* the occlusal surface of the mandible is essentially flat, differing from the condition of *Aussiedraco* in which the mandibular groove is conspicuously raised, relative to the alveolar borders (for revised alveolar measurements of *Aussiedraco*, see Table S2).

In both *Ferrodraco* and QM F44423 the first mandibular tooth pair is vertical and not procumbent. However, QM F44423 differs from *Ferrodraco* in other aspects of its dentition: for example, the teeth of QM F44423 are more robust as indicated by the mesiodistal length and labiolingual width of the preserved alveoli. Furthermore, the first tooth pair in QM F44423 are labiolingually closer to one another than in *Ferrodraco*, which is not unexpected given that the transverse width of the mandible is greater in the latter. Moreover, the tooth count in QM F44423 is higher than that of *Ferrodraco* based on comparisons with similar jaw lengths (QM F44423 preserves 8 alveoli on a 13 cm length fragment, whereas *Ferrodraco* preserves 7 alveoli up to 13 cm). These differences in the dentition and tooth count seem to support the interpretation that QM F44423 and *Ferrodraco* are distinct taxa, occupying slightly different ecological niches. This is unsurprising, given that QM F44423 and *Ferrodraco* are separated in time (upper Albian versus Cenomanian–lowermost Turonian), inhabited different paleoenvironments (inland sea versus floodplain), and likely consumed different types of prey.

A jaw fragment, WAM 68.5.11 from the Molecap Greensand (Cenomanian–Coniacian) at Molecap Hill Quarry, near Gingin in Western Australia, was described by Kear et al. (2010) as a possible ornithocheirid (sensu Unwin 2003) or anhanguerid (sensu Kellner 2003b). The fragmentary nature of WAM 68.5.11 precludes the determination of whether it is an upper or lower jaw (Kear et al., 2010). The fact that the spacing between the alveoli is greater than the diameter of each alveolus excludes WAM 68.5.11 from the Archaeopterodactyloidea (sensu Kellner, 2003b) and Istiodactylidae (Kear et al., 2010). A scalloped jawline, as a consequence of raised alveolar borders is observed in both anhanguerians and targaryendraconians, but absent in the Boreopteridae, Lonchodraconidae, and *Ornithocheirus simus* (Pêgas et al., 2019). The alveoli are anterolaterally oriented, labiolingually compressed, widely spaced and variable in size; all of these features are consistent with the predominantly Early Cretaceous and geographically widespread Ornithocheiridae (Kear et al., 2010). Given its general morphology, the interpretation of WAM 68.5.11 as an ornithocheirid (sensu Unwin, 2001) is tentatively supported here. If this interpretation is correct, it might constitute the youngest ornithocheirid known anywhere in the world; however, given that the age of this unit is poorly constrained, a Cenomanian age is likely: the youngest undoubted record of an ornithocheirid pterosaur is a partial wing from the late Cenomanian of northeastern Mexico (Frey et al., 2020).

Given that WAM 68.5.11 cannot be positively identified as either a maxilla or dentary, comparisons with *Ferrodraco* are limited. However, based on the degree of inflation of the alveolar borders, it is likely that this specimen represents a taxon closely related to *Ferrodraco* or *Mythunga*, possibly within Tropeognathinae or Coloborhynchinae. The interalveolar spacing in WAM 68.5.11 of 22.5 mm is similar to the spacing between the 8th and 9th alveoli preserved on the left dentary of *Ferrodraco* (22 mm).

Given that the total tooth count and tooth density of WAM 68.5.11 cannot be determined, it would be premature to identify WAM 68.5.11 as a jaw fragment near or posterior to the mandibular symphysis, based on comparisons with *Ferrodraco*.

Recently, two isolated teeth, LRF 759 and LRF 3142, preserved as natural, non-precious opal casts in the Griman Creek Formation, were described by Brougham et al. (2017). These authors identified these teeth as pterosaurian, specifically regarding them as indeterminate members of the pterodactyloid clade Anhangueria (sensu Rodrigues and Kellner, 2013). Both teeth are labiolingually compressed, slightly lingually recurved with an oval cross-section, and similar in length to those of *Mythunga camara* (Brougham et al., 2017). Moreover, the authors suggested that the teeth were located mesially within the tooth row, on the basis of their large and elongate crowns.

The dentition of *Ferrodraco* is similar to LRF 759 and LRF 3142 in that both bear fine apicobasal striae; however, the teeth of *Ferrodraco* are not ornamented with pits or longitudinal grooves near the base of the tooth, as observed in LRF 759 (Brougham et al., 2017). As indicated by Table S1, as well as Figures S5–S8, there can be considerable variation in the dentition of a single anhanguerid individual. Variation in dentition may also be influenced by the age of that tooth and is dependent on when that tooth will be replaced.

Although LRF 759 and LRF 3142 are similar in terms of their apicobasal height to the dentition of *Mythunga*, as noted by Brougham et al. (2017), the mesiodistal length of the opalized teeth are perhaps more similar to those of *Ferrodraco* (Table 1) based on their alveolar diameters. This would seem to indicate that these teeth are not as robust as those preserved in *Mythunga*, and are more similar overall to those in *Ferrodraco*. This is not unexpected, given that the Griman Creek Formation is (at least in part) equivalent in age to the middle part of the Winton Formation (Bell et al., 2019). It can then be assumed that the diets and ecological niches filled by pterosaurs derived from the Cenomanian-aged Griman Creek and Winton formations are more similar to one another, than to those of pterosaurs from the upper Albian Toolebuc Formation.

A cervical vertebra, SAM P41968, lacking most of its neural arch and incomplete across the zygapophyses, was found in the upper Albian Toolebuc Formation near Boulia (Kellner et al., 2010). The anteroposterior length of centrum: transverse width at centrum mid-length ratio of this vertebra was <2.5, thereby excluding it from the Azhdarchidae and Archaeopterodactyloidea (Kellner et al., 2010). Kellner et al. (2010) regarded SAM P41968 as similar to *Anhanguera piscator* on the basis of its strongly developed lateral pneumatic foramina and the presence of postexapophyses. The similar morphologies of cervical vertebra 3 to 7 in members of the Anhangueridae, Istiodactylidae and *Pteranodon* means that the precise phylogenetic position of SAM P41968 is difficult to determine (Kellner et al., 2010). Based on its gross morphology, which compares favorably with the aforementioned taxa, Kellner et al. (2010) concluded that SAM P41968 represents a mid-cervical vertebra of an ornithocheiroid. In the only published figure of the cervical vertebra, the scale bar (10 mm) was erroneously given as 100 mm.

Although five partial cervical vertebrae are known from *Ferrodraco*, only three of these can be meaningfully compared with SAM P41968. The only cervical vertebra of *Ferrodraco* that preserves a partial cotyle is cervical vertebra B. Although the cotyle is obscured by adherent matrix, the articular surface is clearly circular, whereas in SAM P41968 the cotyle is triangular in outline (narrowing ventrally). The articular surface of the cotyle of SAM P41968 is much smaller than that of *Anhanguera* sp. (AMNH 22555; Wellnhofer, 1991c). SAM P41968 also possesses a well-developed, lateral pneumatic foramen, as in cervical vertebra B of *Ferrodraco*; however, that of the latter cannot be seen in dorsal view as it has been infilled with matrix. The cotyle is

slightly dorsally deflected relative to the condyle in both SAM P41968 and cervical vertebra B of *Ferrodraco*. The floor of the neural canal is only visible in cervical vertebra B in the *Ferrodraco* holotype specimen; although adherent ironstone partly obscures this feature, its morphology and transverse width is similar to that of SAM P41968.

Of the five partial cervical vertebrae preserved in *Ferrodraco*, only three preserve exapophyses: cervical vertebrae A, C, and D. Of these three, cervical vertebra A bears the most resemblance to SAM P41968 in terms of the angle of the exapophysis relative to the condyle. Given that the angle of the exapophysis relative to the centrum changes along the vertebral column, based on comparisons with *Ferrodraco* and *Anhanguera* sp. (AMNH 22555; Wellnhofer, 1991c), we agree with Kellner et al. (2010) that SAM P41968 is a mid-cervical vertebra of an anhanguerian pterosaur. SAM P41968 differs from cervical vertebra A of *Ferrodraco* in that the exapophyses are narrower in the former; given that the small-sized trabeculae are visible on the centrum and exapophyses of SAM P41968, it is unlikely that this is a taphonomic artifact. Both cervical vertebra A and SAM P41968 preserve near-elliptical condyles (Kellner et al., 2010), with the latter more strongly compressed dorsoventrally.

One of the first pterosaur fossils formally described from Australia was a left scapulocoracoid (QM F10612), in which the scapula and coracoid are fused, indicating an osteologically mature pterosaur (Molnar and Thulborn, 1980). The scapulocoracoid bears some resemblance to *Pteranodon* (Eaton, 1910) and *Anhanguera* (Wellnhofer, 1988, 1991a) in possessing a posterior process and a 'bridge' between the scapula and coracoid located medial to the glenoid (Molnar and Thulborn, 1980). QM F10612 (Fig. 12A–C) can be assigned to Pteranodontoidea, as the coracoid is larger than the scapula (Kellner, 2003c). Moreover, the suboval form of the proximal (glenoid) articulation surface suggests a pteranodontoid (Kellner, 2003c); in more plesiomorphic taxa, the glenoid articular face is more elongate in form (Molnar and Thulborn, 2007). Molnar and Thulborn (2007) regarded the scapulocoracoid as that of a taxon related to *Anhanguera* (although they incorrectly gave the specimen number as QM F10613). The ratio of the preserved scapula to coracoid length is ca. 0.8 (Molnar and Thulborn, 2007). On the basis of the general form of the glenoid, QM F10612 bears resemblance to *Anhanguera* sp. (AMNH 22555; Wellnhofer, 1991c), with the V-shaped fossa of the dorsolateral surface of the scapula located between the posterior process and anterior moiety of the scapula (Molnar and Thulborn, 2007).

Given that the scapulocoracoid preserved in the *Ferrodraco* holotype specimen is solely represented by a glenoid fossa, comparisons with QM F10612 are somewhat limited. The suture between the scapula and coracoid are not visible in *Ferrodraco* whereas an obliterated suture is present in QM F10612. QM F10612 differs from that of *Ferrodraco* in that the anterior portion of the supraglenoidal buttress projects more anteriorly. However, it should be noted that the anterior portion of the supraglenoidal buttress in *Ferrodraco* has been partially eroded, revealing the internal trabeculae. Moreover, the posterior part of the supraglenoidal buttress in *Ferrodraco* is reduced when compared with QM F10612. Given that the cortical bone is still preserved in the posterior section of the supraglenoidal buttress, this is a clear difference in the morphology of the two scapulocoracoids and not a result of erosion. *Ferrodraco* is similar to QM F10612 in that the articular face of the glenoid is suboval, as noted by Fletcher and Salisbury (2010). However, the articular face in *Ferrodraco* does not appear as deeply curved in comparison to QM F10612. This is suggestive of a greater range of motion in *Ferrodraco*; however, it is also worth noting that the influence of ontogeny on the scapulocoracoid of anhanguerian pterosaurs is poorly understood. Although the posterior surface of the lower tubercle in *Ferrodraco* is

incomplete, when compared with QM F10612 the lower tubercle in the latter slopes distally.

A complete but anteroposteriorly flattened wing metacarpal, NMV P197962 (Fig. 13A–F), discovered at Slashers Creek Station (east of Boulia, Queensland) in exposures ascribed to the Toolebuc Formation, was described by Kellner et al. (2010). These authors suggested that it belonged to an individual with a wingspan of ca. 4 m, based on comparisons with *Anhanguera piscator* (Kellner and Tomida, 2000) and *Santanadactylus pricei* (AMNH 22552; Wellnhofer 1991c). Although the shaft and proximal end of NMV P197962 have been crushed, the distal end is three-dimensionally preserved. In their original description, Kellner et al. (2010) concluded that NMV P197962 shared more features with the Anhangueridae (sensu Kellner [2003b]; equivalent to Ornithocheirae sensu Andres et al. [2014]) than with other members of the Pteranodontoidea (Kellner and Tomida, 2000; Wellnhofer, 1985), based on the position of the pneumatic foramen. NMV P197962 is interpreted here as a member of the Ornithocheirae sensu Andres et al. (2014); however, whether it is an anhanguerid sensu Andres et al. (2014), is not certain. The specimen is 212 mm long, with four small depressions on its anterior surface, interpreted as tooth marks and evidence of scavenging prior to fossilization (Kellner et al., 2010).

The preservation of NMV P197962 is similar to that of the left metacarpal IV of *Ferrodraco*, inasmuch as the proximal articular surface and the majority of the shaft have been anteroposteriorly flattened, whereas the distal end is three-dimensionally preserved. Kellner et al. (2010) suggested that the distal end is more resistant to crushing than the rest of the metacarpal, as it is denser here than elsewhere. Although the left metacarpal IV of *Ferrodraco* is anteroposteriorly flattened, synchrotron data indicate that the distal end is not noticeably denser than other parts of this element. As preserved, the maximum width of the distal articular surface of NMV P197962 is 34.3 mm (Kellner et al., 2010; Table 1), whereas this measurement in *Ferrodraco* is 29 mm. Although this would seem to suggest that NMV P197962 is larger overall, the preserved proximodistal length of NMV P197962 is 212 mm (as opposed to 205 mm in *Ferrodraco*). The fact that both elements have suffered anteroposterior flattening, and that the proximal articular surface of the left metacarpal IV of *Ferrodraco* is distorted when compared with the right, precludes further meaningful comparisons between NMV P197962 and *Ferrodraco*.

The proximal end of a left metacarpal IV, QM F44321 (Fig. 12D–H), was recovered from the upper Albian Toolebuc Formation, northeast of Boulia from a horizon stratigraphically higher than the 'fish hash' limestone (Fletcher and Salisbury, 2010). QM F44321 was assigned to Ornithocheiridae (sensu Unwin 2001) by Fletcher and Salisbury (2010), on the basis that it was most similar to metacarpals known from Anhanguera spp. and superficially resembled those described from the Cambridge Greensand. These authors noted that its morphology, specifically the tuberculum and associated sulcus, is distinct from that of any described species (Fletcher and Salisbury, 2010); however, as noted by Fletcher and Salisbury (2010) the fourth metacarpal is not known for *Ornithocheirus*.

Given that the left metacarpal IV of *Ferrodraco* has been anteroposteriorly flattened, comparisons between QM F44321 and *Ferrodraco* are based on the right metacarpal IV. As noted by Fletcher and Salisbury (2010) most of the cortical bone and possibly some fine details have been lost in QM F44321, as a result of erosion.

The general morphology of QM F44321 is interpreted here as representative of its true morphology, given that the tuberculum is more pronounced with respect to the cranioventral and craniodorsal ridges. Moreover, small circular trabeculae are preserved on the dorsal portion of the proximal articular surface of QM F44321, similar to the condition observed in the right metacarpal

FIGURE 12. Pterosaur postcranial remains derived from the upper Albian Toolebuc Formation. **A–C**, left scapulocoracoid, QM F10612 in **A**, posterior, **B**, lateral and **C**, anterior views. **D–H**, proximal end of a left metacarpal IV, QM F44321 in **D**, proximal; **E**, anterior; **F**, dorsal; **G**, posterior; and **H**, ventral views. **I–M**, distal end of a left wing phalanx, QM F44312 in **I**, dorsal; **J**, posterior; **K**, ventral; **L**, anterior; and **M**, distal views. All photographs taken by S.F.P. Scale bar equals 10 mm.

FIGURE 13. Pterosaur right metacarpal IV from the upper Albian Toolebuc Formation NMV P197962 in **A**, proximal; **B**, posterior; **C**, ventral; **D**, anterior; **E**, dorsal; and **F**, distal views. All photographs taken by A.H.P. Scale bar equals 20 mm.

IV of *Ferrodraco*. The rest of the proximal articular surface has been more heavily eroded, as indicated by the exposure of larger, rectangular trabeculae (Fig. 12D). Nevertheless, the proximal articular surface of QM F44321 appears well ossified and is interpreted here as that of a subadult or adult individual. The proximal articular surface of *Ferrodraco* is larger both anteroposteriorly and dorsoventrally than QM F44321, and differs in that the former appears more rectangular in cross section. In posterior view, the proximal articular surface in both QM F44321 and *Ferrodraco* gently slopes ventrally; however, it is more inclined in *Ferrodraco*. An anteroposteriorly elongate shelf is visible in proximal view near the proximal cranioventral ridge in QM F44321, and is level with the ventral part of the proximal anterior sulcus. In this regard, this element is similar to that of *Santanadactylus araripensis* (BSP 1982 I 89; Wellnhofer, 1985) which also possesses an anteroposteriorly elongate shelf in the same position as observed in QM F44321. By contrast, *Ferrodraco* does not possess an analogous shelf on its proximal articular surface. Moreover, the proximal craniodorsal ridge in *Ferrodraco* is well-developed relative to that of QM F44321. Variation in the proximal articular surface between QM F44321 and *Ferrodraco* is perhaps indicative of differences in the degree of rotation between the distal syncarpals and the wing metacarpal.

The proximal cranioventral ridge (= proximal cranioventral crest) is longer ventrally in QM F44321 than in *Ferrodraco*. In contrast, the proximal tuberculum (= cranioproximal crest) and the proximal craniodorsal ridge (= proximal craniodorsal crest) are more pronounced in *Ferrodraco*. Moreover, the dorsal part of the proximal cranial sulcus is more pronounced in *Ferrodraco* than in QM F44321. *Ferrodraco* also differs from other anhanguerians (e.g., *Santanadactylus pricei* [AMNH 22552; Wellnhofer 1991c], *Santanadactylus araripensis* [BSP 1982 I 89; Wellnhofer, 1985], *Santanadactylus araripensis* [BSP 1987 I 66; Wellnhofer, 1991c], *Santanadactylus pricei* [BSP 1980 I 120; Wellnhofer, 1985]) in that the tuberculum, proximal anteroventral crest and proximal anterodorsal crest project posteriorly such that the three features are approximately level with one another, in proximal view. Given that the proximal articular surface of metacarpal IV varies between specimens referred to the same species (e.g., AMNH 22552 and BSP 1980 I 120, both referred to *Santanadactylus pricei* [Wellnhofer, 1985; Wellnhofer, 1991c]), the taxonomic significance of metacarpal IV among anhanguerian pterosaurs remains unclear. Moreover, the influence of ontogeny on the morphology of the proximal articular surface of metacarpal IV is poorly understood among anhanguerian pterosaurs. At the distal end, the transverse cross-sectional shape of QM F44321 is oval, such that the transverse cross section is dorsoventrally elongate. Unfortunately, the distal end of the right metacarpal IV in *Ferrodraco* has been anteroposteriorly flattened, such that the transverse cross-sectional shape cannot be determined with certainty.

The distal portion of a wing phalanx, QM F44312 (Fig. 12I–M), was discovered in the upper Albian Toolebuc Formation on Dunluce Station (between Hughenden and Richmond) and described by Fletcher and Salisbury (2010) as cf. *Anhanguera*. The authors regarded QM F44312 as the distal end of either wing phalanx I or II. QM F44312 was assigned to the Ornithocheiridae (sensu Unwin, 2001) on the basis of the morphology of the cross-sectional shape of the shaft and distal articular head, both of which bear some resemblance to *Santanadactylus pricei* (Wellnhofer, 1985), as well as the apparent absence of pneumatic foramina (Fletcher and Salisbury, 2010). It is possible that erosion to the anterior margin and a major fracture along the mid-shaft have destroyed any diagnostic features that were present. Fletcher and Salisbury (2010) did not specify whether QM F44312 was a left or right wing phalanx; however, based on comparisons with *Santanadactylus pricei* (Wellnhofer, 1991c), QM F44312 is from the left.

The distal end of a wing phalanx is also present in *Ferrodraco*. Although incomplete, the maximum width of this element is 22 mm (Pentland et al., 2019:table 1). Given that the proximal end of phalanx IV-1 is almost complete, with a maximum width of 54 mm (Pentland et al., 2019:table 1), it is likely that the distal wing phalanx corresponds to manual phalanx IV-1. If this interpretation is correct, and the proximal end of phalanx IV-1 in *Ferrodraco* is comparable in size to that of *Santanadactylus pricei* (Wellnhofer, 1985), the maximum width of the distal end of phalanx IV-1 can be estimated for *Ferrodraco*. Given that Wellnhofer (1985) reconstructed the maximum width of the distal end of phalanx IV-1 in *Santanadactylus pricei* as 32 mm, we can assume that approximately one third of the distal end of phalanx IV-1 in *Ferrodraco* is missing. By contrast, the maximum width of QM F44312 is given as 29 mm (Fletcher and Salisbury, 2010:table 3). Based on comparisons with *Santanadactylus pricei* and *Ferrodraco*, QM F44312 is tentatively identified here as the distal end of manual phalanx IV-1. In distal view, QM F44312 is oval in cross section (Fletcher and Salisbury, 2010) and in this regard it is similar to that of *Santanadactylus pricei* (Wellnhofer, 1985). *Ferrodraco* differs from *Santanadactylus pricei* and QM F44312 in that although the distal end is incomplete, the posterior surface is defined by a distinct margin. Although the posterior surface in *Ferrodraco* preserves most of its cortical bone, the posterior surface appears somewhat

FIGURE 14. Life restoration of *Ferrodraco lentoni*. Illustration by R.J.D.

depressed. Therefore, the cross-sectional shape of the distal end of phalanx IV-1 in *Ferrodraco* might be somewhat exaggerated because of crushing.

As noted by Fletcher and Salisbury (2010), the anterior portion of the distal articular surface in QM F44312 is eroded relative to the posterior portion. However, based on comparisons with *Santanadactylus pricei* in which Wellnhofer (1985) noted that the posterior portion of the distal articular surface slopes posteriorly, the morphology of QM F44312 is representative of its true morphology. Based on the size and shape of the trabeculae visible on the distal articular surface in QM F44312, relatively little has been lost. In contrast, the distal articular surface of *Ferrodraco* preserves much larger trabeculae, suggesting that the latter is more eroded in comparison to the QM F44312.

The Australian pterosaur fauna is so far limited to the Cretaceous and dominated by indeterminate members of the Ornithocheirae (sensu Andres et al., 2014), with the majority of the described material derived from the upper Albian Toolebuc Formation. *Mythunga* has been most recently resolved as a member of the Ornithocheirinae and the sister taxa to *Ferrodraco*, whereas *Aussiedraco* has been recovered as the sister taxon to a clade comprising *Barbosania* (Elgin and Frey, 2011) and *Targaryendraco* (Pêgas et al., 2019). Together, *Aussiedraco*, *Barbosania*, and *Targaryendraco* form the clade Targaryendraconidae (Pêgas et al., 2019). QM F44423, a partial mandibular symphysis, anatomically overlaps with *Aussiedraco* and has been regarded by Fletcher and Salisbury (2010) and more recently, Pêgas et al. (2019), as most similar to *Aussiedraco* and *Targaryendraco*. However, Pêgas et al. (2019) note that it cannot be referred to the Targaryendraconidae, as it does not demonstrate all of the synapomorphies of that clade. Moreover, QM F44423 differs from the Boreopteridae, the Lonchodraconidae, and *Ornithocheirus simus* in that the alveolar borders are raised such that the jawline appears scalloped (Pêgas et al., 2019). QM F44423 is identified here as an indeterminate member of the Ornithocheirae (sensu Andres et al., 2014) and likely represents a taxon distinct from the four named species of Australian pterosaur. However, we refrain from erecting a new taxon based on the limited material available.

Of the postcranial material from the Toolebuc Formation that can be directly compared with *Ferrodraco* (Fig. 14), three specimens are morphologically distinct. They include QM F10612, a three-dimensionally preserved scapulocoracoid; QM F44321, the proximal end of a left metacarpal IV; and QM F44312, the distal end of a wing phalanx. Although QM F10612 differs from *Ferrodraco* in terms of the morphology of the supraglenoidal buttress and the articular face of glenoid, we cannot rule out the influence of ontogeny. QM F10612 is referred to the Pteranodontoidea. Similarly, although the proximal articular surface of QM F44321 is markedly different to that of *Ferrodraco*, this varies among members of the Anhangueria (see Fletcher and Salisbury, 2010: fig. 5). We follow Fletcher and Salisbury (2010) and refer QM F44321 to the Ornithocheiridae (sensu Unwin, 2001), approximately equivalent to the Ornithocheirae (sensu Andres et al., 2014). QM F44312 also differs from that of *Ferrodraco*, and is referrable to the Ornithocheirae (sensu Andres et al., 2014).

While three elements are clearly distinct from those of *Ferrodraco*, it cannot be ruled out that some of the postcranial material discussed might belong to either *Mythunga*, *Aussiedraco*, or *Thapunngaka*. NMV P197962, an anteroposteriorly flattened yet complete wing metacarpal, attributed to a pterosaur with a wingspan of 4 m could also belong to either *Mythunga*, *Aussiedraco*, or *Thapunngaka*. Given that NMV P197962 is crushed, comparisons with *Ferrodraco* are somewhat limited; however, the wing metacarpal can be referred to the Ornithocheirae (sensu Andres et al., 2014). Of the postcranial material formally described from the Albian Toolebuc Formation, SAM P41968 is the only specimen that can be referred to the less inclusive Anhangueria. Moreover, based on comparisons with *Ferrodraco*

and the cervical series of *Anhanguera* sp. (AMNH 22555), SAM P41968 is regarded as a mid-cervical vertebra. Anhanguerian pterosaurs have also been reported from the Cenomanian Griman Creek Formation, based on isolated teeth described by Brougham et al. (2017). More recently Pêgas et al. (2019) has questioned the anhanguerian affinities of these teeth, suggesting that referral to the Ornithocheirae might be better, rather than the Anhangueria.

CONCLUSION

Ferrodraco lentoni represents the most complete Australian pterosaur, and the only specimen known from a partial skeleton. The detailed description of this specimen (particularly the postcranial skeleton), and renewed phylogenetic appraisal of *Ferrodraco*, demonstrate unequivocally that it belongs in the family Anhangueridae (sensu Holgado and Pêgas, 2020). The previously proposed close relationship between *Ferrodraco* and *Mythunga* is robustly supported, as is their phylogenetic affinity with *Tropeognathus*. However, upon comparing the results of our analyses, the precise position of *Ferrodraco* and *Mythunga* within Anhangueridae still remains uncertain. Rigorous comparison of the postcranial remains of *Ferrodraco lentoni* with isolated pterosaur remains previously reported from Australia has demonstrated that several of the latter elements are morphologically distinct; whether these are related to *Mythunga camara*, *Aussiedraco molnari*, *Thapunngaka shawi*, or an as yet undetected taxon at present remains uncertain. Nevertheless, the presence of numerous anhanguerian lineages in the Early to mid-Cretaceous of northeast Australia provides some context for the Australian pterosaur fauna, and suggests their diversity has been greatly underestimated.

ORCID

Adele H. Pentland http://orcid.org/0000-0003-4827-1996
Stephen F. Poropat http://orcid.org/0000-0002-4909-1666
Matt A. White http://orcid.org/0000-0002-4765-0356
Samantha L. Rigby http://orcid.org/0000-0002-7403-0910
Ruairidh J. Duncan http://orcid.org/0000-0002-5348-5043

LITERATURE CITED

Andres, B., J. Clark, and X. Xu. 2014. The earliest pterodactyloid and the origin of the group. Current Biology 24:1011–1016.

Bell, P. R., F. Fanti, L. J. Hart, L. A. Milan, S. J. Craven, T. Brougham, and E. Smith. 2019. Revised geology, age, and vertebrate diversity of the dinosaur–bearing Griman Creek Formation (Cenomanian), Lightning Ridge, New South Wales, Australia. Palaeogeography, Palaeoclimatology, Palaeoecology 514:655–671.

Bennett, S. C., and J. A. Long. 1991. A large pterodactyloid pterosaur from the Late Cretaceous (Late Maastrichtian) of Western Australia. Records of the Western Australian Museum 15:435–443.

Brougham, T., E. T. Smith, and P. R. Bell. 2017. Isolated teeth of Anhangueria (Pterosauria: Pterodactyloidea) from the Lower Cretaceous of Lightning Ridge, New South Wales, Australia.

Buffetaut, E., A. ÓSI, and E. Prondvai. 2011. The pterosaurian remains from the Grünbach Formation (Campanian, Gosau Group) of Austria: a reappraisal of 'Ornithocheirus buenzeli'. Geological Magazine 148:334–339.

Campos, D. d. A., and A. Kellner. 1985. Panorama of the flying reptiles study in Brazil and South America. Anais da Academia Brasileira de Ciências 57:453–466.

Colbert, E. H. 1969. Jurassic pterosaur from Cuba. American Museum Novitates 2370:1–26.

Collini, C. A. 1784. Sur quelques Zoolithes du Cabinet d'Histoire naturelle de SASE Palatine and de Bavière, à Mannheim. Acta Academiae Theodoro Palatinae, Mannheim, Pars Physica 5:58–103.

Cope, E. D. 1871. On two new ornithosaurians from Kansas. Proceedings of the American Philosophical Society 12:420–422.

Cuvier, G. 1809: Mémoire sur le squelette fossile d'un reptile volant des environs d'Aichstedt, que quelques naturalistes ont pris pour un oiseau, et dont nous formons un genre de Sauriens, sous le nom de Ptero-Dactyle. Paper presented at the Annales du Muséum national d'Histoire Naturelle, Paris, 1809.

Dubey, V., and K. Narain. 1946. A note on the occurrence of Pterosauria in India. Current Science 15:287–288.

Eaton, G. F. 1910. Osteology of *Pteranodon*. Memoirs of the Connecticut Academy of Arts and Sciences 2:38.

Elgin, R. A., and E. Frey. 2011. A new ornithocheirid, *Barbosania gracilirostris* gen. et sp. nov.(Pterosauria, Pterodactyloidea) from the Santana Formation (Cretaceous) of NE Brazil. swiss Journal of Palaeontology 130:259.

Fletcher, T. L., and S. W. Salisbury. 2010. New pterosaur fossils from the Early Cretaceous (Albian) of Queensland, Australia. Journal of Vertebrate Paleontology 30:1747–1759.

Frey, E., D. M. Martill, and M.-C. Buchy. 2003. A new crested ornithocheirid from the Lower Cretaceous of northeastern Brazil and the unusual death of an unusual pterosaur. Geological Society, London, Special Publications 217:55–63.

Frey, E. D., Stinnesbeck, W., Martill, D. M., Rivera-Sylva, H. E. and Múzquiz, H. P. 2020. The geologically youngest remains of an ornithocheirid pterosaur from the late Cenomanian (Late Cretaceous) of northeastern Mexico with implications on the paleogeography and extinction of Late Cretaceous ornithocheirids. Palaeovertebrata 43:1–12.

Goloboff, P. A., J. S. Farris, and K. Nixon. 2008. TNT, a free program for phylogenetic analysis. Cladistics 24:774–86.

Gray, A. R. G., M. McKillop, and J. L. McKellar. 2002. Eromanga basin stratigraphy; pp. 30–56 + references and figures in J. J. Draper (ed.), Geology of the Cooper and Eromanga basins, Queensland, Department of Natural Resources and Mines, Brisbane.

Hammer, W. R., and W. J. Hickerson. 1994. A crested theropod dinosaur from Antarctica. Science–AAAS–Weekly Paper Edition–including Guide to Scientific Information 264:828–830.

Holgado, B., and R. V. Pêgas. 2020. A taxonomic and phylogenetic review of the anhanguerid pterosaur group Coloborhynchinae and the new clade Tropeognathinae. Acta Palaeontologica Polonica, 65:743–761.

Hone, D. W., D. Naish, and I. C. Cuthill. 2012. Does mutual sexual selection explain the evolution of head crests in pterosaurs and dinosaurs? Lethaia 45:139–156.

Jacobs, M. L., D. M. Martill, N. Ibrahim, and N. Longrich. 2019. A new species of *Coloborhynchus* (Pterosauria, Ornithocheiridae) from the mid-Cretaceous of North Africa. Cretaceous Research 95:77-88.

Jain, S. L. 1974. Jurassic pterosaur from India. Geological Society of India 15:330–335.

Jell, P. A. 2013. Geology of Queensland. Geological Survey of Queensland.

Kaup, J. J. 1834. Versuch einer Eintheilung der Saugethiere in 6 Stämme und der Amphibien in 6 Ordnungen. Isis 3:311–315.

Kear, B. P., G. L. Deacon, and M. Siverson. 2010. Remains of a Late Cretaceous pterosaur from the Molecap Greensand of Western Australia. Alcheringa 34:273–279.

Kellner, A. 2003a. Comments on the phylogeny of the Pterodactyloidea. Rivista del Museo Civico di Scienze Naturali 'Enrico Caffi 22:31–37.

Kellner, A. W. 2003b. Pterosaur phylogeny and comments on the evolutionary history of the group. Geological Society, London, Special Publications 217:105–137.

Kellner, A. W. A. 2003c. Comments on the phylogeny of the Pterodactyloidea. Rivista del Museo Civico di Scienze Naturali "E. Caffi" di Bergamo 22:31–37.

Kellner, A. W., and Y. Tomida. 2000. Description of a new species of Anhangueridae (Pterodactyloidea) with comments on the pterosaur fauna from the Santana Formation (Aptian–Albian), northeastern Brazil. National Science Museum Monographs 17:ix–137.

Kellner, A. W., M. B. Aguirre-Urreta, and V. A. Ramos. 2003. On the pterosaur remains from the Río Belgrano formation (Barremian), Patagonian Andes of Argentina. Anais da Academia Brasileira de Ciências 75:487–495.

Kellner, A. W., T. Rodrigues, and F. R. Costa. 2011. Short note on a pteranodontid pterosaur (Pterodactyloidea) from western Queensland, Australia. Anais da Academia Brasileira de Ciências 83:301–308.

Kellner, A. W., T. H. Rich, F. R. Costa, P. Vickers-Rich, B. P. Kear, M. Walters, and L. Kool. 2010. New isolated pterodactyloid bones from the Albian Toolebuc Formation (western Queensland, Australia) with comments on the Australian pterosaur fauna. Alcheringa 34:219–230.

Kellner, A. W., D. A. Campos, J. M. Sayao, A. A. Saraiva, T. Rodrigues, G. Oliveira, L. A. Cruz, F. R. Costa, H. P. Silva, and J. S. Ferreira. 2013. The largest flying reptile from Gondwana: a new specimen of *Tropeognathus* cf. *T. mesembrinus* Wellnhofer, 1987 (Pterodactyloidea, Anhangueridae) and other large pterosaurs from the Romualdo Formation, Lower Cretaceous, Brazil. Anais da Academia Brasileira de Ciências 85:113–135.

Kellner, A. W. A., T. Rodrigues, F. R. Costa, L. C. Weinschütz, R. G. Figueiredo, G. A. D. Souza, A. S. Brum, L. H. S. Eleutério, C. W. Mueller, and J. M. Sayão. 2019. Pterodactyloid pterosaur bones from Cretaceous deposits of the Antarctic Peninsula. Anais da Academia Brasileira de Ciências 91.

Lee, Y.-N. 1994. The Early Cretaceous pterodactyloid pterosaur *Coloborhynchus* from North America. Palaeontology 37:755–764.

Lü, J. 2010. A new boreopterid pterodactyloid pterosaur from the Early Cretaceous Yixian Formation of Liaoning Province, northeastern China. Acta Geologica Sinica (English edition) 84:241–246.

Mader, B. J., and A. W. A. Kellner. 1999. A new anhanguerid pterosaur from the Cretaceous of Morocco. Boletim do Museu Nacional, Rio de Janeiro, Nova Serie, Geologia, 45: 1–11.

Maddison, W. P., & Maddison, D. R. 2018. Mesquite: a modular system for evolutionary analysis. Version 3.6.

Marsh, O. C. 1872. Discovery of additional remains of Pterosauria with descriptions of two new species. American Journal of Science:241–248.

Marsh, O. C. 1876. Principal characters of American pterodactyls. American Journal of Science:479–480.

Mawson, J., and A. Smith Woodward. 1907. On the Cretaceous formation of Bahia (Brazil), and on vertebrate fossils collected therein. Quarterly Journal of the Geological Society 63:128–NP.

Molnar, R., and R. Thulborn. 1980. First pterosaur from Australia. Nature 288:361–363.

Molnar, R. E., and R. A. Thulborn. 2007. An incomplete pterosaur skull from the Cretaceous of north-central Queensland, Australia. Arquivos do Museu Nacional, Rio de Janeiro 65:461–470.

Myers, T. S. 2010. A new ornithocheirid pterosaur from the Upper Cretaceous (Cenomanian–Turonian) Eagle Ford Group of Texas. Journal of Vertebrate Paleontology 30:280–287.

Myers, T. S. 2015. First North American occurrence of the toothed pteranodontoid pterosaur *Cimoliopterus*. Journal of Vertebrate Paleontology 35:e1014904.

Pêgas, R. V., B. Holgado, and M. E. C. Leal. 2019. On *Targaryendraco wiedenrothi* gen. nov. (Pterodactyloidea, Pteranodontoidea, Lanceodontia) and recognition of a new cosmopolitan lineage of Cretaceous toothed pterodactyloids. Historical Biology:1–15.

Pentland, A. H., and S. F. Poropat. 2019. Reappraisal of *Mythunga camara* Molnar and Thulborn, 2007 (Pterosauria,

Pterodactyloidea, Anhangueria) from the upper Albian Toolebuc Formation of Queensland, Australia. Cretaceous Research 2019:151–169.

Pentland, A. H., S. F. Poropat, T. R. Tischler, T. Sloan, R. A. Elliott, H. A. Elliott, J. A. Elliott, and D. A. Elliott. 2019. *Ferrodraco lentoni* gen. et sp. nov., a new ornithocheirid pterosaur from the Winton Formation (Cenomanian–lower Turonian) of Queensland, Australia. Scientific Reports 9:13454.

Pinheiro, F. L., and T. Rodrigues. 2017. *Anhanguera* taxonomy revisited: is our understanding of Santana Group pterosaur diversity biased by poor biological and stratigraphic control? PeerJ 5: p.e3285.

Plieninger, F. 1901. Beiträge zur Kenntniss der Flugsaurier (Pterodactlyus kochi [Germanodactylus], Pteranodon). Palaeontographica 48:65–90.

Price, L. 1953. A presença de Pterosauria no Cretáceo Superior do Estado da Paraíba. Notas Preliminares e Estudos 71:1–10.

Reck, H. 1931. Die deutschostafrikanischen Flugsaurier (Pterodactylus brancai [Tendaguripterus]). Centralblatt für Mineralogie, Geologie und Paläontologie 1931:321–336.

Richards, T. M., P. E., Stumkat, and S. W. Salisbury. 2021. A new species of crested pterosaur (Pterodactyloidea, Anhangueridae) from the Lower Cretaceous (upper Albian) of Richmond, North West Queensland, Australia. Journal of Vertebrate Paleontology 41: e1946068.

Rodrigues, T., and A. W. Kellner. 2008. Review of the pterodactyloid pterosaur *Coloborhynchus*. Zitteliana:219–228.

Rodrigues, T., and A. W. A. Kellner. 2010. Note on the pterosaur material described by Woodward from the Recôncavo Basin, Lower Cretaceous, Brazil. Revista Brasileira de Paleontologia 13:159–164.

Rodrigues, T., and A. W. A. Kellner. 2013. Taxonomic review of the *Ornithocheirus* complex (Pterosauria) from the Cretaceous of England. PenSoft Publishers LTD.

Tucker, R. T., E. M. Roberts, Y. Hu, A. I. Kemp, and S. W. Salisbury. 2013. Detrital zircon age constraints for the Winton Formation, Queensland: contextualizing Australia's Late Cretaceous dinosaur faunas. Gondwana Research 24:767–779.

Unwin, D. M. 2001. An overview of the pterosaur assemblage from the Cambridge Greensand (Cretaceous) of Eastern England. Fossil Record 4:189–221.

Unwin, D. M. 2003. On the phylogeny and evolutionary history of ptero-saurs. Geological Society, London, Special Publications 217:139–190.

Unwin, D. M., and W. D. Heinrich. 1999. On a pterosaur jaw from the Upper Jurassic of Tendaguru (Tanzania). Fossil Record 2:121–134.

Veldmeijer, A. J. 2003. Description of *Coloborhynchus spielbergi* sp. nov.(Pterodactyloidea) from the Albian (Lower Cretaceous) of Brazil. Scripta Geologica 125:e139.

Veldmeijer, A. J., M. Signore, and H. Meijer. 2005. *Brasileodactylus* (Pterosauria, Pterodactyloidea, Anhangueridae); an update. Cranium 22:45–56.

Vila Nova, B. C., J. M. Sayão, V. H. M. L. Neumann, and A. W. A. Kellner. 2014. Redescription of *Cearadactylus atrox* (Pterosauria, Pterodactyloidea) from the Early Cretaceous Romualdo Formation (Santana Group) of the Araripe Basin, Brazil. Journal of Vertebrate Paleontology 34:126–134.

Vine, R., and W. Jauncey. 1964. Mackunda 1: 250 000 Geological Series Sheet SF 54–11. Bureau of Mineral Resources, Canberra.

Vine, R., R. Day, D. Casey, E. Milligan, M. Galloway, and N. Exon. 1967. Revised nomenclature of the Rolling Downs Group, Eromanga and Surat Basins. Queensland Government Mining Journal 68:144–151.

Wang, X.-L., and Z.-H. Zhou. 2003. Two new pterodactyloid pterosaurs from the Early Cretaceous Jiufotang Formation of western Liaoning, China. Vertebrata PalAsiatica 41:34–49.

Wang, X., A. W. Kellner, S. Jiang, and X. Cheng. 2012. New toothed flying reptile from Asia: close similarities between early Cretaceous ptero-saur faunas from China and Brazil. Naturwissenschaften 99:249–257.

Wellnhofer, P. 1985. Neue Pterosaurier aus der Santana-Formation der Chapada do Araripe, Brasilien. Palaeontographica, Abteilungen A 187:105–182.

Wellnhofer, P. 1987. New crested pterosaurs from the Lower Cretaceous of Brazil. Mitteilungen der Bayerischen Staatssammlung für Paläontologie und historische Geologie 27:175–186.

Wellnhofer, P. 1988. Terrestrial locomotion in pterosaurs. Historical Biology 1:3–16.

Wellnhofer, P. 1991a. The illustrated encyclopedia of pterosaurs. Crescent Books.

Wellnhofer, P. 1991b. The Santana Formation pterosaurs, pp. 351–370. In Maisey, J. G. (ed.), Santana Fossils: an Illustrated Atlas. Neptune City, NJ: T.F.H. Publications.

Wellnhofer, P. 1991c. Weitere Pterosaurierfunde aus der Santana-Formation (Apt) der Chapada do Araripe, Brasilien. Palaeontographica Abteilung A:43–101.

Young, C.-C. 1964. On a new pterosaurian from Sinkiang, China. Vertebrate Palasiatica 8:221–225.